

Louisiana State University

LSU Scholarly Repository

LSU Master's Theses

Graduate School

2014

Bioavailability of Alpha-Tocopherol Entrapped in Poly (lactide-co-glycolide) (PLGA) and PLGA-Chitosan Nanoparticles

Lacey Caroline Simon

Louisiana State University and Agricultural and Mechanical College

Follow this and additional works at: https://repository.lsu.edu/gradschool_theses



Part of the [Engineering Commons](#)

Recommended Citation

Simon, Lacey Caroline, "Bioavailability of Alpha-Tocopherol Entrapped in Poly (lactide-co-glycolide) (PLGA) and PLGA-Chitosan Nanoparticles" (2014). *LSU Master's Theses*. 2290.

https://repository.lsu.edu/gradschool_theses/2290

This Thesis is brought to you for free and open access by the Graduate School at LSU Scholarly Repository. It has been accepted for inclusion in LSU Master's Theses by an authorized graduate school editor of LSU Scholarly Repository. For more information, please contact gradetd@lsu.edu.

BIOAVAILABILITY OF ALPHA-TOCOPHEROL ENTRAPPED IN POLY (LACTIDE-CO-
GLYCOLIDE) (PLGA) AND PLGA-CHITOSAN NANOPARTICLES

A Thesis

Submitted to the Graduate Faculty of the
Louisiana State University and
Agricultural and Mechanical College
in partial fulfillment of the
requirements for the degree of
Master of Science

in

The Department of Biological and Agricultural Engineering

by

Lacey Simon

B.S., Louisiana State University, 2012

May 2014

This is dedicated to my parents, Ray and Pat Simon.

Acknowledgments

God has blessed me beyond measure with the people and opportunities necessary to complete this endeavor. I am most grateful for my family who has selflessly given their time, love, and financial support throughout my entire education. I would also like to thank my major advisor, Dr. Sabliov, who has never stopped believing in me. Dr. Sabliov's mentorship went beyond that of an advisor. She not only provided unparalleled insight and guidance relative to my research, but she was happy to make time to advise me about all aspects of life. I want to thank my committee members Dr. Hayes and Dr. Monroe for offering their unique perspectives and challenging me to strive for excellence.

The completion of this project would not be possible without the time and dedication of Dr. Rhett Stout. Dr. Stout spent countless hours, early mornings, late nights, and weekends helping me collect samples from the animals. I feel so blessed to have worked with someone with such expertise who voluntarily gave his time to this project. His patience and wisdom are one of a kind, and I will be forever in debt of his generosity. I also want to thank Dr. Carlos Astete who has mentored me in the areas of particle synthesis and characterization. I owe much of my success to his instruction and patience.

Finally, I would like to thank my friends and colleagues who have offered their support and wisdom whenever possible, especially Toni Borel, Thanida Chuacharoen, Daniel Bourgeois, and Sara Navarro.

Table of Contents

Acknowledgments.....	iii
List of Abbreviations	v
Abstract	vi
Chapter 1 Introduction	1
1.1 Vitamins & Health Benefits	1
1.2 Pharmacokinetics	2
1.3 Objectives.....	9
Chapter 2 The Effect of Nanoparticles Properties, Detection Method, Delivery Route, and Animal Model on Poly (lactic-co-glycolic) Acid Nanoparticles Biodistribution in Mice and Rats	11
2.1 Introduction	11
2.2 Organ-by-Organ Biodistribution Analysis	12
2.3 Discussion	25
2.4 Conclusion.....	28
Chapter 3 Bioavailability of Alpha-tocopherol Entrapped in Poly (lactide-co-glycolide) (PLGA) and PLGA-Chitosan Nanoparticles	30
3.1 Introduction	30
3.2 Materials.....	31
3.3 Methods.....	32
3.4 Results	36
3.5 Discussion	42
Chapter 4 Conclusions and Future Work.....	45
4.1 Conclusions	45
4.2 Future Work	45
References.....	47
Appendices.....	51
Appendix A Particle Characterization	51
Appendix B Pharmacokinetic Data	61
Appendix C Permission to Publish.....	65
Vita.....	67

List of Abbreviations

α T	α -Tocopherol
AUC	Area Under the Curve
Chi	Chitosan
C _{max}	Maximum concentration
dT	Delta-tocopherol
i.v.	Intravenous
NPs	Nanoparticles
PBS	Phosphate Buffer Saline
PDI	Poly Dispersity Index
PK	Pharmacokinetic
PLGA	Poly (Lactide-co-Glycolide)
PVA	Polyvinyl Alcohol
T _{max}	Time of maximum concentration

Abstract

Alpha-tocopherol (α T) is a hydrophobic, antioxidant molecule shown to prevent or retard the effects of free radicals associated with diseases. It is hypothesized that the bioavailability of α T can be improved when entrapped in PLGA (Poly lactide-co-glycolide) and PLGA-Chi (PLGA-Chitosan) nanoparticles and that the mucoadhesive properties of chitosan may enhance absorption more than PLGA alone. PLGA and PLGA-Chi NPs synthesized with PVA as surfactant were characterized by measuring entrapment efficiency, size, PDI, and zeta potential when suspended in DI water. Nanoparticle physical stability was evaluated via NP exposure to environmental pH ranging from 2.5-9. Chemical stability of entrapped α T was also investigated by exposing particles to simulated GI (gastro-intestinal) environments for 48 hours, and release kinetics were measured in these conditions for 72 hours. Pharmacokinetic studies were conducted by administering PLGA (α T) NPs, PLGA-Chi (α T) NPs, and free α T in a flour, water, and corn oil slurry via oral gavage in rats. Blood samples were collected over 72 hours. Entrapment efficiency was $95.4 \pm 9.85\%$, for PLGA NPs and $77.95 \pm 1.51\%$ for PLGA-Chi NPs. The size and zeta potential of the two particle systems were 97.87 ± 2.63 nm and -36.2 ± 1.31 mV for PLGA(α T) NPs, and 134 ± 2.05 nm and 38.0 ± 2.90 mV for PLGA-Chi (α T) nanoparticles in DI water. PLGA(α T) NPs showed a change in size of only 4 nm in the pH range of 2.5-9, while PLGA-Chi(α T) nanoparticles revealed a 46 nm change in size in pH 2.5-9. Entrapped α T showed no degradation in GI conditions over 48 hours. Release kinetics also showed no release of the α T from either NP system over 72 hours. Bioavailability of nanodelivered α T was improved as indicated compared to the free α T up to 170% and 121% for PLGA and PLGA-Chi NPs, respectively. These findings revealed that both delivery systems increased bioavailability of α T, but chitosan did not improve uptake of α T, as hypothesized.

1.1.2 Alpha-tocopherol—Challenges in Absorption

Although health benefits associated with intake of α T are a result of its chemical structure, the structure of α T is partly responsible for challenges in absorption following oral administration. Specifically, low mucosal permeability, low solubility of the compound, premature elimination prior to absorption, and chemical and enzymatic instability in the GI tract are major barriers in absorption of lipophilic vitamins such as α T (Murugesu et al., 2011). According to Barker et al. (2003), one challenge in proper absorption associated with the structure of α T is the accelerated degradation as a result of its low oxidative stability when exposed to heat and oxygen (Song et al., 2009). According to Murugesu et al. (2011), the efficiency of absorption of tocopherols was reported to be approximately 36% in normal subjects, however the conditions were not reported. This absorption efficiency is highly dependent on the chemical form and the nature of the matrix in which the α T is suspended or dissolved (Yang & McClements, 2013).

1.1.3 Alpha-tocopherol—Metabolism

The fate of vitamin E within the body is linked to dietary fat. Absorption in the intestine requires bile salts, pancreatic enzymes, and adequate fat to be present. In general for fat-soluble vitamins, formation of micelles containing dietary lipids, emulsified in the presence of bile salts, is necessary for absorption (Lodge, 2005). The bioaccessibility of lipophilic bioactives such as α T has been reported to increase as the total amount of mixed micelles increases. This bioaccessibility also depends on the nature of the mixed micelles present after lipid digestion (Yang & McClements, 2013). Because of this route of absorption, variable absorption is likely depending on fed/fasted status of individual (Barker et al., 2003). Once vitamin E is internalized into the enterocyte, it is packaged into chylomicrons, and it enters circulation via the lymphatic system. Once the chylomicrons are in circulation, the chylomicron triglycerides are subjected to hydrolysis via lipoprotein lipase. The result of this process is the transfer of lipids, including α T, to peripheral tissues (Lodge, 2005).

1.2 Pharmacokinetics

In order to reach optimum efficacy, a bioactive such as α T must have a high bioavailability (Yang & McClements, 2013). The FDA defines bioavailability as the rate and extent to which the active drug ingredient or therapeutic moiety is absorbed from a drug product and becomes available at the site of drug action (Cohn, 1997). Bioavailability is studied quantitatively in a field called pharmacokinetics. Pharmacokinetics (PK) is the study of drug disposition in the body with a focus on changes in drug plasma concentration (Brenner & Stevens, 2009). The rates of four processes—absorption, distribution, metabolism, and elimination—determine the rise and fall of plasma concentrations of any given drug. Absorption refers to the movement of a drug into the bloodstream, and the rate of absorption relies on the physical characteristics

of the drug and its formulation. Distribution is the process of the drug leaving the blood stream and going into organs and tissues, while metabolism refers to the biotransformation of a drug primarily in the liver. Elimination of a drug is the process of excretion of the parent compound or its metabolites, typically by the kidneys (Brenner & Stevens, 2009).

Numerous barriers associated with absorption of drugs are unique to oral administration. For example, when a drug is administered orally, it must be absorbed through a layer of epithelial cells with tight junctions. In addition, drugs must also avoid first-pass biotransformation which occurs when orally administered drugs are absorbed from the gut and reach the liver through the hepatic portal vein. A fraction of the drug can then be metabolized in the liver before reaching systemic circulation, reducing oral bioavailability of the parent compound (Brenner & Stevens, 2009). Quantitative pharmacokinetics is used to determine the efficiency of a formulation to by-pass barriers in absorption such as first-pass biotransformation and passage through tight junctions of the epithelial cells. To determine the oral bioavailability of a particular drug, the area under the curve (AUC) of the drug's plasma concentration-time curve is needed. This curve represents the relationship between drug plasma concentrations with respect to time following an acute dose of the drug (Figure 1.2).

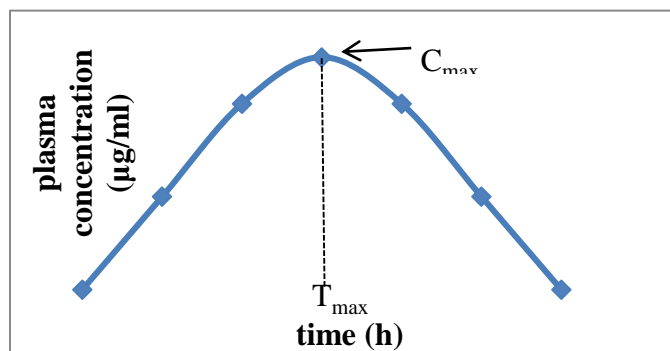


Figure 1.2. In the plasma concentration-time curve of a drug, the Y axis is the linear scale of drug plasma concentration, typically in $\mu\text{g/ml}$, and the X axis represents time, typically in hours.

From the drug plasma concentration curve, parameters of pharmacokinetics can be obtained. The maximum concentration (C_{max}), the time needed to reach the maximum concentration (T_{max}), and the AUC are the most important parameters to determine pharmacokinetic properties of a formulation. The AUC represents a measure of the total amount of drug absorbed during the time course, and this value is useful for comparing the bioavailability of different formulations. Specifically, oral bioavailability of a certain drug is determined by dividing the AUC_{oral} by the $\text{AUC}_{\text{IV (intravenous)}}$ (Brenner & Stevens, 2009). Relative bioavailability of a certain drug can be determined by dividing the AUC

of two different delivery systems of the same drug. Pharmacokinetic properties are important to discover before any drug formulation can be made commercially available.

1.2.1 Alpha-tocopherol Delivery Systems

Studies have been conducted with the intent of enhancing the bioavailability of α T by circumventing the challenges associated with its oral delivery. One group saw an 18% increase in bioavailability when using α T-loaded Ca-pectinate microcapsules when compared to delivery of free α T (Song et al., 2009). This biopolymeric system was based on the use of natural polysaccharides as a safe and effective drug delivery matrix that would aid in protection of accelerated degradation of α T due to its low oxidative stability and poor solubility in water. The same group previously studied Ca-alginate microcapsules, but the initial burst release limited the application of this microparticle system for delivery of alpha-tocopherol.

An alternative, Ca-pectinate gel microcapsules were produced by Ca-induced ionotropic gelation of low methoxyl pectin, producing a nontoxic, biocompatible, biodegradable, and structurally strong product. Male rats were given a dose of 10 mg α T/kg body weight in free form or entrapped in Ca-pectinate microcapsules. When free α T was given, an immediate increase in plasma α T concentration was observed, and the C_{\max} occurred before 5 h following administration (Figure 1.3). In contrast, the Ca-pectinate microcapsules showed a much slower increase in plasma concentration of α T, with a C_{\max} occurring at 9 h after administration. These findings reinforce the notion that micro and nano delivery systems have the potential to increase bioavailability of a bioactive as well as change the pharmacokinetic profile (Song et al., 2009).

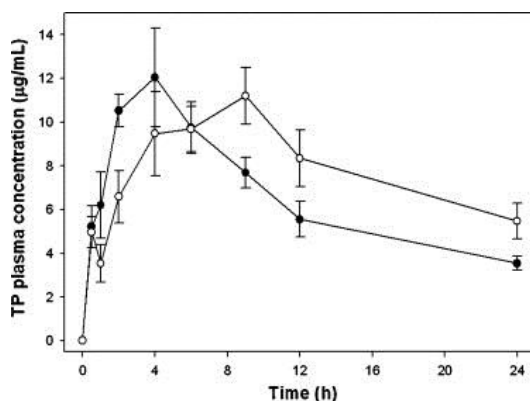


Figure 1.3. The plasma concentration-time curve as determined in rats represents the control α T (●) and α T delivered in Ca-pectinate microparticles (○) (Song et al., 2009).

Gelucire 44/14 preparations were reported to double the oral bioavailability of α T compared to commercially available α T (Barker et al., 2003). The goal of this study was to reduce variable absorption of α T depending on fed/fasted status of an individual and also to formulate an appropriate formulation suitable for drugs liquid at room temperature

(Barker et al., 2003). Gelucire 44/14 was chosen because of its proven improvement of bioavailability and increased dissolution rate. The compound is one of a family of lipid-based excipients (the Gelucires) which comprises a mixture of pegylated fatty acid esters and glycerides, and the two numbers of their names correspond to the approximate melting point and HLB value, respectively. This particular study involved comparative oral bioavailability in human volunteers between a Gelucire 44/14 formulation of 300 IU α T and an equivalent commercial capsule based on an oily solution. The T_{\max} was the same for both commercial and Gelucire 44/14 formulations, which occurred at 10 hours following administration (Figure 1.4).

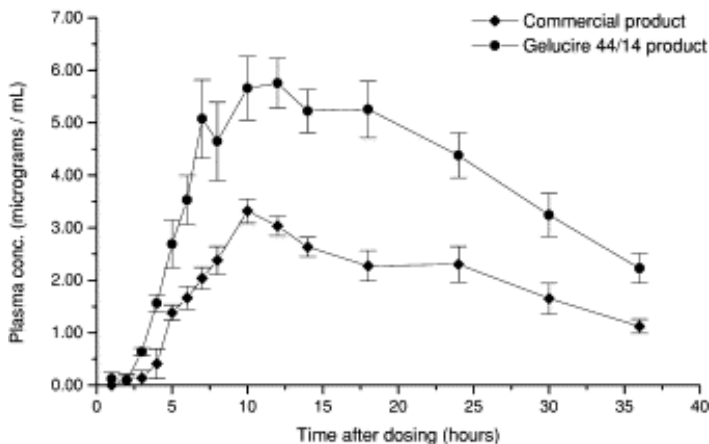


Figure 1.4. The comparison of human plasma concentration over time is shown for α T in Gelucire 44/14 preparation (top curve) and commercial α T product (bottom curve) (Barker et al., 2003).

The author reported a two-fold increase in absorption of the formulated preparation over the control, lending confidence to their premise that Gelucire 44/14 formulation enhances bioavailability (Barker et al., 2003).

In 2010, a study successfully enhanced α T bioavailability by 160% via a nano-emulsion system (Hatanaka et al., 2010). The purpose of the nano-emulsion system was to improve intracellular uptake, stability, and solubility of active substances, in particular, α T. The researchers compared several liquid formulations of α T which were prepared by a mechanochemical method, and the phases were composed of α T and medium chain triglyceride (MCT) for the lipid phase and decaglycerol monooleate, lecithin, glycerol, and DI water for the aqueous phase. Rats were given a dose of 30 mg α T/kg body weight in the nano-emulsion form or in free form as a control. Plasma levels of α T varied greatly between the nano-emulsion formulation and the control of α T suspended in MCT (Figure 1.5) (Hatanaka et al., 2010).

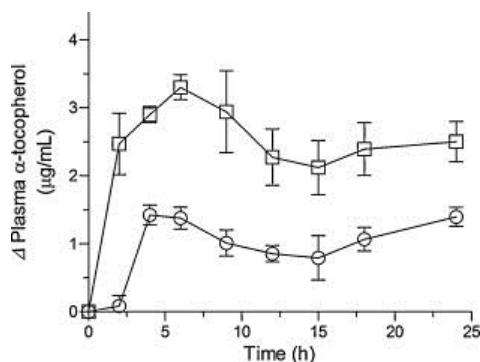


Figure 1.5. The pharmacokinetic profiles in rats of a control α T solution in MCT (o) and a novel nano-emulsion preparation (\square) are represented (Hatanaka et al., 2010).

1.2.2 Nanoparticles as a Delivery System

Nanomedicine is defined by the European Science Foundation as nanometer size scale complex systems consisting of at least two components, one of which being the active ingredient. Most current research involving nanotechnology explores behavior of particles 1-200 nm in diameter, but the size of particles used in drug delivery may range from 2-1000 nm (Plapied et al., 2011). Nanoparticles used for delivery of therapeutic agents must meet certain criteria. For example, the nanoparticles must be stable, non-toxic, non-immunogenic, biodegradable, and should be applicable to numerous molecules such as proteins, vaccines, nucleic acids, or small drugs such as α T (Plapied et al., 2011).

Nanoparticles offer a plethora of advantages to the field of oral drug delivery. The growing list of advantages of nanomedicine includes the reduce fed/fasted variable absorption, improved dose proportionality, potential to minimize drug attrition rates, increased rate of absorption, ability to overcome GI window of absorption, delivery of insoluble drugs, targeting of drugs, and transcellular delivery of drugs (Grama et al., 2011). Because of these advantages, nanomedicines have the potential to increase efficacy, specificity, tolerability, and most importantly bioavailability of the corresponding drugs (Plapied et al., 2011).

Recently, synthesis of polymeric nanoparticles as drug delivery vehicles has taken the spotlight due to their pharmaceutical advantages (Grama et al., 2011). Polymeric nanoparticles offer the ability to deliver drugs falling under 4 different classes—Class I (high permeability high solubility), Class II (high permeability low solubility), Class III (low permeability high solubility) and Class IV (low permeability low solubility), and these nanoparticles can protect the therapeutic ingredient from GI degradation, ensuring stability of the drug in the GI tract. In addition to providing protection from harsh chemicals and enzymes in the GI tract, polymeric nanocarriers have the ability to increase oral bioavailability by withstanding first pass metabolism via their lymphatic uptake mechanism (Grama et al., 2011).

1.2.3 PLGA

Polymeric nanoparticles are favored by some over emulsions for drug delivery formulations due to their stability and protection of the entrapped bioactive. Poly (lactide-co-glycolide) (PLGA) (Figure 1.6) is a promising polymer used for nano-entrapment of and delivery of drugs.

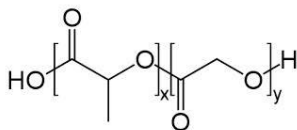


Figure 1.6. The structure of PLGA is composed of alternating lactic acid and glycolic acid monomers (<http://commons.wikimedia.org/wiki/File:PLGA.svg>).

PLGA is a biocompatible synthetic co-polymer that is commercially available, and it degrades into its monomers which are lactic acid and glycolic acid, by-products of the citric acid cycle. Because PLGA has been thoroughly characterized and has FDA approval, it is the most comprehensively researched commercially available polymer (Mittal et al., 2007).

PLGA NPs have been shown to improve oral bioavailability of insoluble compounds in several references. For example, one group studied the effects on oral bioavailability of cyclosporine after entrapment in PLGA nanoparticles stabilized with DMAB (Italia et al., 2007). In this study, male rats were given a dose of cyclosporine entrapped in PLGA nanoparticles or a control called Sandimmune Neoral® via oral gavage of 15 mg/kg body weight. The results of the *in vivo* bioavailability study on PLGA delivery of cyclosporine is shown in Figure 1.7.

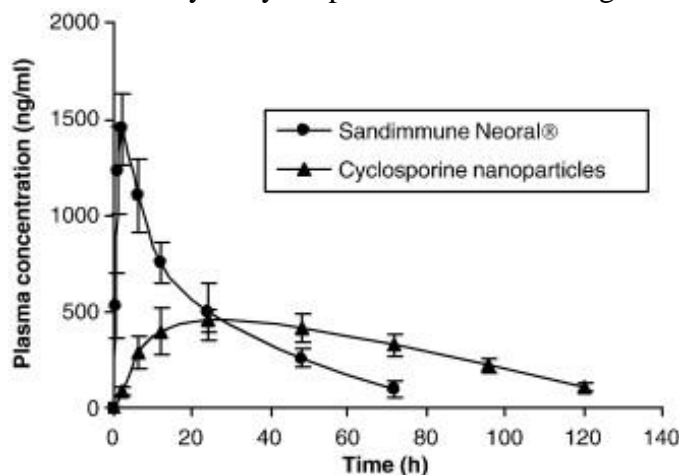


Figure 1.7. The plasma concentration-time curve of cyclosporine delivered in PLGA NPs or in a commercial formulation illustrates the controlled-release of PLGA NPs *in vivo* (Italia et al., 2007).

The pharmacokinetic parameters determined from the plasma concentration-time curve shown in Figure 1.7 are summarized in Table 1.1. According to these results, the cyclosporine-entrapped PLGA NPs enhanced uptake by 19.2%.

Table 1.1. The pharmacokinetic parameters of cyclosporine delivered in rats are summarized (Italia et al., 2007).

Formulation type	C_{\max} (ng/ml)	T_{\max} (h)	$AUC_{0-\infty}$ (ng h/ml)
Sandimmune Neoral®	1448.3 ± 182.4	2	33396.0 ± 4512.9
Cyclosporine NPs	448.5 ± 61.4	24	39806.7 ± 3970.2

All values reported are mean \pm S.D. ($n = 3$).

Similarly, a study by Mittal et al. (2007) was published showing improved bioavailability of estradiol entrapped in PLGA NPs. Estradiol was chosen as the drug of interest because although it has a good oral absorption, it has very low bioavailability (10%) because of first pass metabolism. This study involved estradiol entrapment into PLGA NPs of several different molecular weights and varying lactide:glycolide ratios. Male rats were orally gavaged with the equivalent dose of 1 mg estradiol/ rat, and pure estradiol was administered orally in 0.05% DMSO solution. It is evident from the profile (Figure 1.8) that the plasma concentration profile of estradiol entrapped in PLGA NPs showed a sustained release compared to the control.

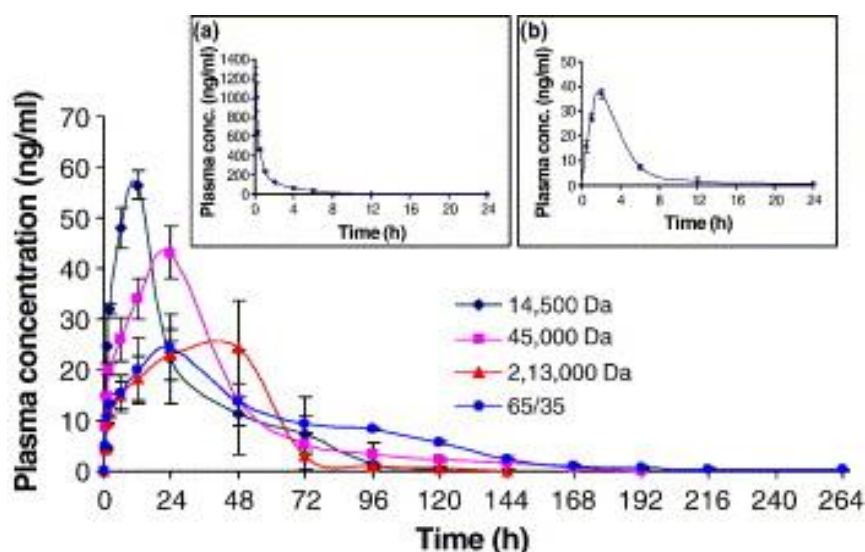


Figure 1.8. The different molecular weights of PLGA NPs with entrapped estradiol show varying pharmacokinetic profiles. The curves determined from the estradiol entrapped in NPs are very different from the curve developed from i.v. administration of the control (a) and oral administration of the control (b) (Mittal et al., 2007).

The 213,000 Da molecular weight PLGA nanoparticles showed a release of estradiol over 6 days with a C_{\max} of 28.55 ng/ml and a T_{\max} of 32 hours. Oral administration of the control only showed a 1 day release profile, with a slightly higher

C_{\max} of 37.08 ng/ml at T_{\max} of 2 hours (Mittal et al., 2007). The author reports that a significant increase ($p < 0.001$) in the AUC values of all the nanoparticle formulations in comparison to the orally delivered control was found (Mittal et al., 2007). Several other groups found increased bioavailability of drugs orally delivered in PLGA NPs: doxorubicin (363%) (Grama et al., 2011), amphotericin B (793%) (Grama et al., 2011), and curcumin (2583%) (Grama et al., 2011), (2200%) (Tsai, et al., 2011), (1560%) (Khalil et al., 2012).

1.2.4 Chitosan

Chitosan is an additional material of interest in nano-entrapment of bioactives for increased bioavailability. Chitosan (Figure 1.9) is formed by N-deacetylation of chitin (Plapied et al., 2011).

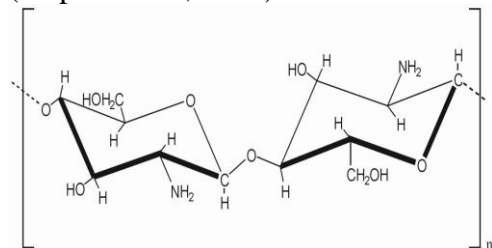


Figure 1.9. Chitosan is an N-deacetylated derivative of chitin.

The beneficial traits of chitosan are its biocompatibility, non-toxic effects, and most importantly, its mucoadhesive properties, and this mucoadhesion is believed to be a result of chitosan's positive zeta potential. Mucoadhesion is important because it is understood that nanocarriers must adhere to the intestinal mucus to cross this mucus layer. The negatively charged intestinal mucosa attracts positively charged particles, making the addition of positively-charged chitosan to PLGA nanoparticles a very promising approach to increase residence time in the GI tract (Plapied et al., 2011).

It is hypothesized that the bioavailability of α T can be improved when entrapped in PLGA and PLGA/Chitosan nanoparticles and that the mucoadhesive properties of chitosan may play a role in enhancing absorption even more so than PLGA alone.

1.3 Objectives

The objectives of this thesis were to conduct a review on biodistribution of PLGA nanoparticles in rats and mice (Chapter 2) and to study the effects of nanodelivery on bioavailability of a model bioactive (Chapter 3).

1.3.2 Biodistribution

Nanotechnology has the potential to change the face of preventative and clinical medicine as it is known today, but in order to utilize the vast applications of these types of delivery systems, they must be completely understood and characterized *in vivo*. Certain particles and bioactives have the potential to be toxic to certain organs and tissues (Mittal et al., 2007) so knowledge of the NP residence time in each respective organ provides direction on how to choose proper delivery systems for specific applications. Many unanswered questions refer to particle behavior, toxicity, and clearance

The objective of Chapter 2 was to address these unknowns based on what has already been published. Specifically, a review was conducted on biodistribution of PLGA NPs delivered in mice and rats. The purpose of the review was to identify correlations between particle biodistribution and NP properties (size), animal model (mice and rats), type of delivery (intravenous vs oral), and detection method (covalently-linked indicator or entrapped indicator). Relative biodistribution of PLGA nanoparticles in various organs over time was also reported. This review is entitled “The effect of nanoparticle properties, detection method, delivery route, and animal model on poly(lactic-co-glycolic) acid nanoparticles biodistribution in mice and rats” and it was published in *Drug Metabolism Reviews* in December of 2013.

1.3.3 Bioavailability

The goal of the study reported in Chapter 3 of this thesis was to investigate the ability of PLGA and PLGA-Chi NPs to improve bioavailability of a model lipophilic bioactive, α T. It was hypothesized that NP systems enhanced bioavailability of α T over that of the free vitamin and that PLGA-Chi NPs were more proficient in improving the α T bioavailability when compared to PLGA NP delivery. PLGA and PLGA-Chi NPs with entrapped α T were synthesized according to an emulsion evaporation method followed by dialysis washing and lyophilization for 48 hours. The NPs were characterized *in vitro* in terms of size, polydispersity index (PDI), zeta potential, release kinetics, chemical stability, and physical stability. Next, the ability of PLGA and PLGA-Chi NPs to improve the bioavailability of the entrapped α T was tested *in vivo*. Both NP systems were gavaged to male rats along with a control of free α T, and the plasma concentration of α T was measured over time. The chosen matrix was a flour-in-water and oil slurry consisting of 30% oil and 70% flour in water. The NPs were suspended in the flour-in-water phase for their delivery, and the free α T was suspended in the oil phase. The AUC determined from the plasma concentration of α T in the rats showed a 270% increase in bioavailability when delivered in PLGA NPs compared to α T delivered in free form. The AUC, and thus bioavailability, of the PLGA-Chi delivered α T was not statistically different than the AUC of the PLGA NP delivered α T. This study proved that PLGA NPs is a viable and promising delivery system for lipophilic bioactives with poor bioavailability due to the chemical and physical protection provided by the NPs.

Chapter 2 The Effect of Nanoparticles Properties, Detection Method, Delivery Route, and Animal Model on Poly (lactic-co-glycolic) Acid Nanoparticles Biodistribution in Mice and Rats¹

2.1 Introduction

Nanoparticulate delivery systems such as poly(lactic-co-glycolic) acid (PLGA) nanoparticles (NPs) are increasing in popularity because they promise to overcome numerous biological barriers associated with drug administration (Cartiera, et al., 2009). Over the past ten years, research on PLGA NPs as drug delivery systems has increased exponentially. Specifically, studies involving intravenous (i.v.) or oral delivery of PLGA NPs in mice and rats have been continuously published in an attempt to understand implications of PLGA NP behavior *in vivo* on the toxicity of the delivery system and effectiveness of the entrapped drugs. For example, eight review papers published on polymeric NPs were identified, with a focus on biodistribution, biotoxicity, and targeting (Acharya et al., 2010; Acharya and Sahoo, 2011; Aggarwal, et al., 2009; Danhier et al., 2012; Fredenberg et al., 2011; Gaumet, et al., 2008; Owens and Peppas, 2006; Phillips, et al., 2010)

While these review papers contain useful and pertinent information relative to NP properties and their specific influence on biodistribution, none of them thoroughly discusses PLGA NPs and their behavior *in vivo*. There is a critical need to compile and analyze the abundance of research published on biodistribution of PLGA NPs as a function of their physico-chemical properties in an effort to map-out translocation of PLGA NP to various organs following oral and i.v. administration. Knowledge of NP biodistribution is required to both correlate potential biotoxicity of NPs with their properties and to improve the effectiveness of the NPs in treatment or prevention of certain diseases.

It was the goal of this review paper to compile the available data on PLGA NP biodistribution and to quantitatively present NP presence in major tissues over time in rats and mice exposed, either orally or intravenously to a single dose of NPs. The effect of type of animals used, method employed for NP detection, and NP properties on the observed biodistribution trends were also discussed. To reach this goal, a literature search was conducted on Science Direct and Web of Science using the following key words: biodistribution, NPs, PLGA, polymeric NPs, mice, rats.

This initial search resulted in 3600 publications, which were then limited to ten papers which included information on PLGA NP uptake by major organs, including liver, brain, heart, spleen, kidney, and lungs. Each publication found on PLGA biodistribution was summarized, highlighting the NP system, method of testing, and major biodistribution results. Emphasis was placed on the particle system, including size, zeta

¹ This chapter previously appeared as Simon, Lacey, C. M. Sabliov, “The effect of nanoparticle properties, detection method, delivery route, and animal model on poly(lactic-co-glycolic) acid nanoparticles biodistribution in mice and rats” in Drug Metabolism Reviews in December 2013. It is reprinted by permission of Informa Healthcare.

potential, surfactants used, loaded drugs, and any surface modifications involved in the study. The method used to track NPs *in vivo* was identified and categorized; these methods included detection of fluorescence, detection of radioactivity, or detection of the loaded drug. After identifying the specific drug parameters, the procedures for drug administration (i.v. or oral) and animal model (mouse or rat) were reported. Lastly, the percentage dose NP was listed for major organs tested.

2.2 Organ-by-Organ Biodistribution Analysis

The data reported in the featured publications was analyzed with respect to organ uptake of PLGA NPs. In order to normalize all data, particle uptake was converted to percent dose/g determined in each organ. It is noted that in the papers cited in this review, different animals, animal strains, animal ages and animal sexes were used, and sometimes the strain, sex, age was not specified. It is understood that organ weight in rodents is dependent on these listed (or unlisted) specifications. However, due to a lack of specifications in some cases or the inability to identify the organ size for the specific situation reported, in all cases an average value was used (Table 2.1).

Table 2.1. The approximate rat and mouse organ weight (Rat Phenome Database; The Jackson Laboratory).

Organ	mass (g)	
	rat	mouse
spleen	0.5 ¹	0.1 ²
liver	8.5 ¹	1.2 ²
lung	0.9 ¹	0.15 ²
brain	2 ¹	0.4 ²
heart	0.9 ¹	0.13 ²
kidney	1.8 ¹	0.7 ²

Available data was analyzed separately for each organ and results were reported on nanoparticle biodistribution as a function of time, nanoparticle size, type of indicator, and animal model, as follows.

2.2.1 Liver

The percent dose detected per gram of liver was compared across ten different studies reported on oral delivery of PLGA NPs (Tobio, et al., 2000; Yin, et al., 2007) and i.v. delivery of PLGA NPs, (Beletsi, Panagi, and Avgoustakis, 2005; Li, et al., 2001; Mondal, et al., 2010; Parveen and Sahoo, 2011; Saxena, Sadoqi, and Shao, 2006; Snehalatha, et al., 2008; Tosi, et al., 2010; Vergoni, et al., 2009) (Figures 2.1a and 2.1b).

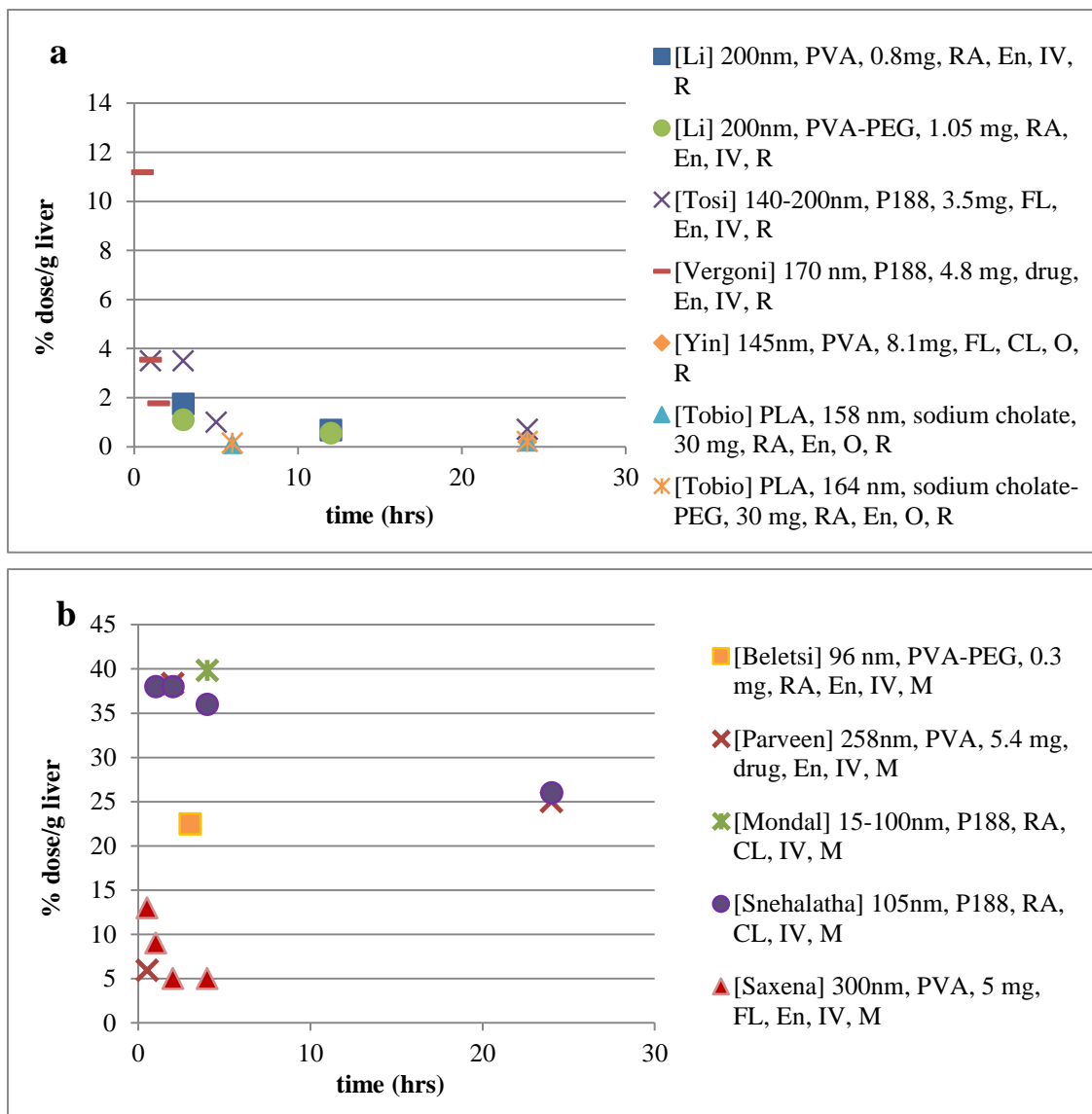


Figure 2.1. Comparative biodistribution of nanoparticles (NPs) in the liver are shown in (a) rats and (b) mice. Data is presented as percent dose per gram of liver with respect to time, after a single dose was administered at time zero. Particle characteristics included in the legend are: [reference], nanoparticle size (mean diameter), surfactant (PVA=poly vinyl alcohol; P188=poloxamer 188, PEG=poly ethylene glycol), NP dose, detection probe (RA=radioactivity, FL=fluorescence, drug=entrapped model drug), location of detection probe (EN=entrapped, CL= covalently linked), method of NP administration (IV=intravenous delivery, O= oral delivery), and animal model (R=rat, M=mouse) (Beletsi, Panagi, and Avgoustakis, 2005; Li, et al., 2001; Mondal, et al., 2010; Parveen and Sahoo, 2011; Saxena, Sadoqi, and Shao, 2006; Snehalatha, et al., 2008; Tobio, et al., 2000; Tosi, et al., 2010; Vergoni, et al., 2009; Yin, et al., 2007).

Time profile

The level of NPs in the liver decreased over a 24 hrs period after a single administration of NPs at time zero in both rats and mice (Figures 2.1a and 1 b). For example, particles of 170 nm delivered intravenously in rats were detected at 11.2% dose/g after thirty minutes following administration, and after 1.5 hours, only 1.8% dose/g was detected in the liver (Vergoni, et al., 2009), (Figure 2.1a). In comparison, for particles of 258 nm, the % dose/g decreased from 38% at 2 hrs after administration to 25% dose/g at 24 hours (Parveen and Sahoo, 2011) (Figure 2.1b). This study was done in mice, and the particles were also administered via i.v. delivery. The drastic decrease over time in both animal models could be associated with rapid uptake of i.v. administered NPs from the circulatory system and then clearance from the liver after administration. When looking at particle content in the liver at 24 hours, all studies done in rats, including (Li, et al., 2001; Tobio et al., 2000; Tosi, et al., 2010; Vergoni, et al., 2009; Yin, et al., 2007) showed almost no detection of particles 24 hours post administration.

The highest detected amount reported was 38% of the administered dose per gram of liver for particles delivered intravenously in mice, (Mondal, et al., 2010; Parveen and Sahoo, 2011; Snehalatha, et al., 2008) (Figure 2.1b). These systems featured particles synthesized with polyvinyl alcohol (PVA) (Parveen and Sahoo, 2011) and poloxamer 188 (P188) (Mondal, et al., 2010; Snehalatha, et al., 2008).

Animal model

It was noted that of the systems showing a high initial uptake, all were administered in a mouse model, (Mondal, et al., 2010; Parveen and Sahoo, 2011; Snehalatha, et al., 2008), and it was also noted that in general, when expressed as % dose/g tissue, NP concentration was higher in mice. That is to be expected, considering that for the same dose of administered NP, the % dose reaching the liver was smaller when dividing by the weight of the rat liver, 6-7 times bigger, on average, than liver of mice. This principle applies to all organs studied in this analysis; kidney, lung, spleen, heart, brain.

To make this point, liver uptake of two particle systems of similar characteristics was compared across two studies, one done in mice and the other one in rats. Li, et al. (2001) tested 200 nm NP in rats and Beletsi, Panagi, and Avgoustakis (2005) tested 96 nm in mice, both applied doses less than 1 mg, and both systems used entrapped radioactivity for detection. The detected amount of particles in the liver from the system delivered in rats was only 1.8% of the administered dose/g liver (Figure 2.1a), whereas the amount detected in mice was 23% dose/g liver (Figure 2.1b). If total % dose/liver were to be compared across animals for these two studies, assuming 1.2 g for the mouse liver and 8.5 g for the rat liver, similar numbers are found 15.3% dose/g liver in rats (Li, et al., 2001) and 15.6% dose/g liver in mice (Saxena, Sadoqi, and Shao, 2006).

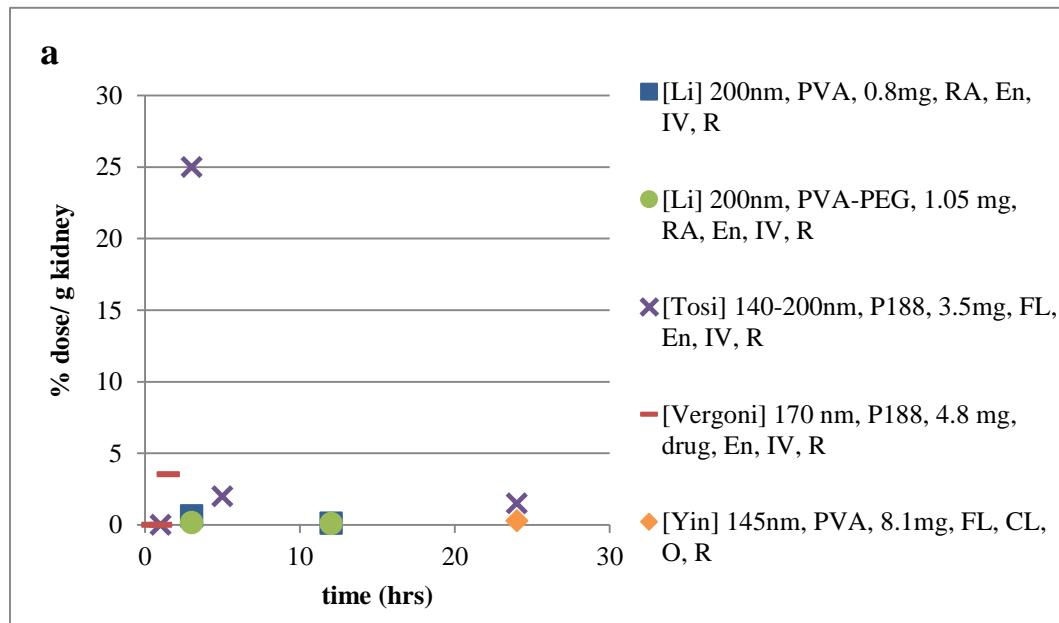
NP size

Particles of comparable sizes showed similar values detected in the liver. For example, particles of 140-200 nm delivered via i.v. delivery in rats were detected between 3.5-1.0% dose/g for the first five hours following administration (Tosi, et al., 2010). Similarly, particles of 170 nm intravenously administered in rats showed uptake of 1.8-3.5% dose/g between 1-1.5 hrs post administration (Vergoni, et al., 2009), (Figure

2.1a). These two systems utilized the same surfactant, mode of administration, animal, similar dose, and location of indicator; one used an entrapped drug for indication, and the other used an entrapped fluorophore. Similarly in mice, two systems of particles each of 100 nm were detected at 36% dose/g (Snehalatha, et al., 2008) and 39.8% dose/g (Mondal, et al., 2010) four hours after i.v. delivery (Figure 2.1b). On the other hand, particles of 300 nm delivered in mice were only detected at 5% dose/g liver 4 hours after i.v. administration (Saxena, Sadoqi, and Shao, 2006) (Figure 2.1b). The differences in the detected NP concentrations with respect to NP size reinforced the notion that smaller particles are taken up at higher concentrations in the liver and the similarity in the uptake of particles of similar sizes builds confidence in the results obtained across various studies.

2.2.2 Kidney

The percent dose detected per gram of kidney was compared across nine different studies for oral delivery (Yin, et al., 2007), and i.v. delivery (Beletsi, Panagi, and Avgoustakis, 2005; Li, et al., 2001; Mondal, et al., 2010; Parveen and Sahoo, 2011; Saxena, Sadoqi, and Shao, 2006; Snehalatha, et al., 2008; Tosi, et al., 2010; Vergoni, et al., 2009) of PLGA NPs in rats (Figure 2.2a) and mice (Figure 2.2b). Uptake of particles for all systems was detected at levels as high as 25% dose/g for rats (Tosi, et al., 2010) (Figure 2.2a) and 16.8% dose/g in mice (Parveen and Sahoo, 2011) (Figure 2.2b), following administration of a single dose of NPs. All systems but one--(Tosi, et al., 2010)--were detected at levels below 4% of the injected dose/g of tissue in rats over a 24 hour period (Figure 2.2a). In mice, all studies reported less than 8% dose/g kidney, with one exception (Parveen and Sahoo, 2011) (Figure 2.2b).



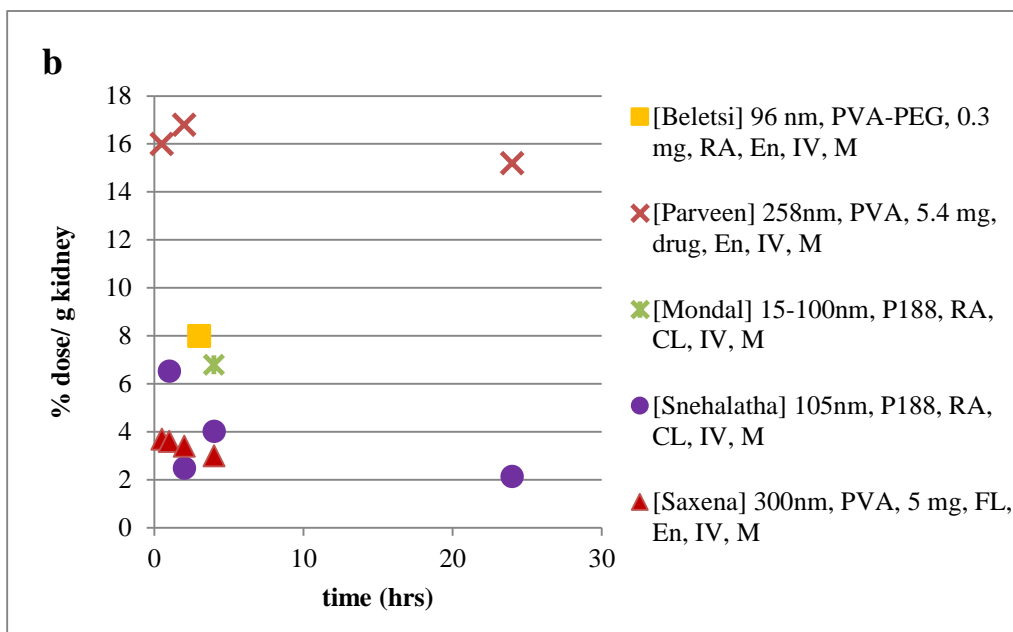


Figure 2.2. Comparative biodistribution of nanoparticles (NPs) in the kidney are shown in (a) rats and (b) mice. Data is presented as percent dose per gram of kidney with respect to time, after a single dose administered at time zero. Particle characteristics included in the legend are: [reference], nanoparticle size (mean diameter), surfactant (PVA=poly vinyl alcohol; P188=poloxamer 188, PEG=poly ethylene glycol), NP dose, detection probe (RA=radioactivity, FL=fluorescence, drug=entrapped model drug), location of detection probe (EN=entrapped, CL= covalently linked), method of NP administration (iv=intravenous delivery, o= oral delivery), and animal model (R=rat, M=mouse) (Beletsi, Panagi, and Avgoustakis, 2005; Li, et al., 2001; Mondal, et al., 2010; Parveen and Sahoo, 2011; Saxena, Sadoqi, and Shao, 2006; Snehalatha, et al., 2008; Tosi, et al., 2010; Vergoni, et al., 2009; Yin, et al., 2007).

Time profile

A gradual decrease in kidney particle content was seen over time, but four of the nine studies showed a significant presence in the kidney even 24 hours after administration (Parveen and Sahoo, 2011; Snehalatha, et al., 2008; Tosi, et al., 2010; Yin, et al., 2007). For example, 25% of the dose/g tissue was detected 3 hours following administration (Tosi, et al., 2010), and 24 hours after administration, 1.5% of the dose/g of tissue still remained (Tosi, et al., 2010) when NPs measuring 140-200 nm were delivered intravenously to rats (Figure 2.2a). Similarly, particles with a mean diameter of 105 nm administered via i.v. delivery to mice were present in the kidney at 6.5% dose/g kidney one hour after administration (Snehalatha, et al., 2008) and 2% dose/g 24 hours post administration (Snehalatha, et al., 2008) (Figure 2.2b).

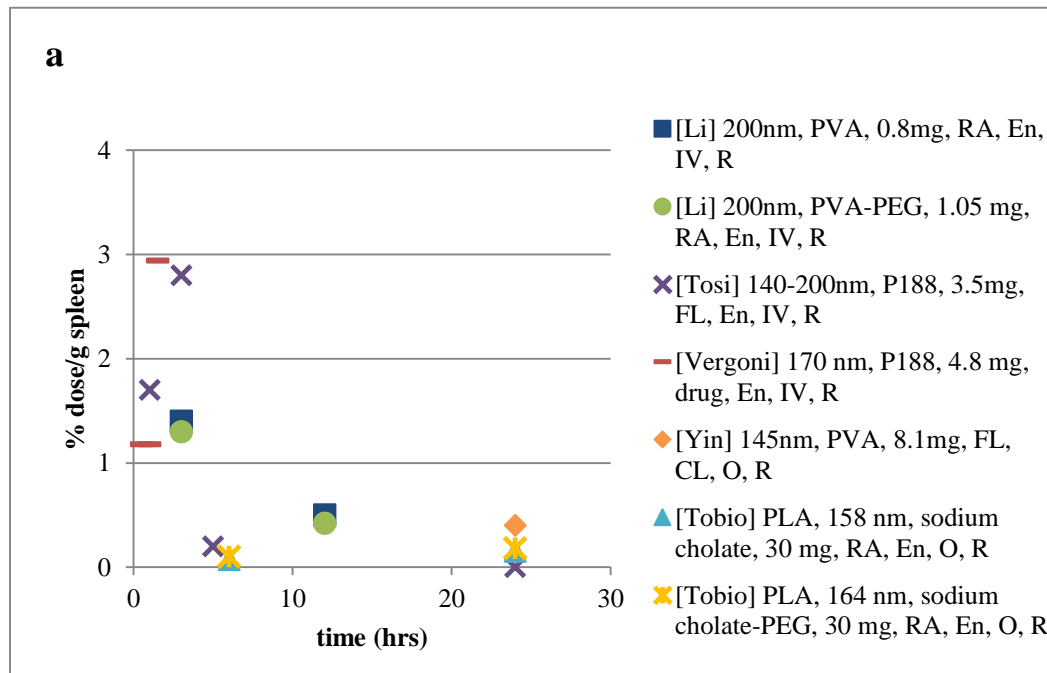
NP size

The data revealed that particle uptake by the kidney was a function of NP size. For example, excluding one outlier of 25% dose/g tissue (Tosi, et al., 2010), particles

with mean diameters between 140 and 200 nm used in i.v. delivery in rats showed an uptake between 3.5% dose/g and 1.5% dose/g between 1.5-24 hours post administration (Tosi, et al., 2010; Vergoni, et al., 2009) (Figure 2.2a). These particles showed a higher uptake in the kidney than did larger particles with a mean diameter of 200 nm also delivered intravenously in rats (0.65% dose/g kidney at 3 hours past administration) (Li, et al., 2001). Following the same pattern, particles of 96 nm intravenously administered in mice were detected at 8% dose/g after 3 hours post administration (Beletsi, Panagi, and Avgoustakis, 2005), and particles of 15-100 nm were detected at 6.8% dose/g 4 hours after administration (Mondal, et al., 2010) (Figure 2.2b). On the other hand, particles of 300 nm intravenously delivered in mice showed only 3% dose/g kidney four hours post administration (Saxena, Sadoqi, and Shao, 2006). Size is perhaps the largest common denominator differentiating uptake patterns between these various particles, but it is important to note that the doses, indicators, and surfactants used were not uniform across studies, and these parameters may also have contributed to observed uptake patterns.

2.2.3 Spleen

Ten papers were used to compare PLGA NP uptake in the spleen when administered in rats (Li, et al., 2001; Tobio, et al., 2000; Tosi, et al., 2010; Vergoni, et al., 2009; Yin, et al., 2007), ((Figure 2.3a) and mice (Beletsi, Panagi, and Avgoustakis, 2005; Mondal, et al., 2010; Parveen and Sahoo, 2011; Saxena, Sadoqi, and Shao, 2006; Snehalatha, et al., 2008) (Figure 2.3b), and all systems but two (Tobio et al., 2000; Yin, et al., 2007) used i.v. delivery of NPs.



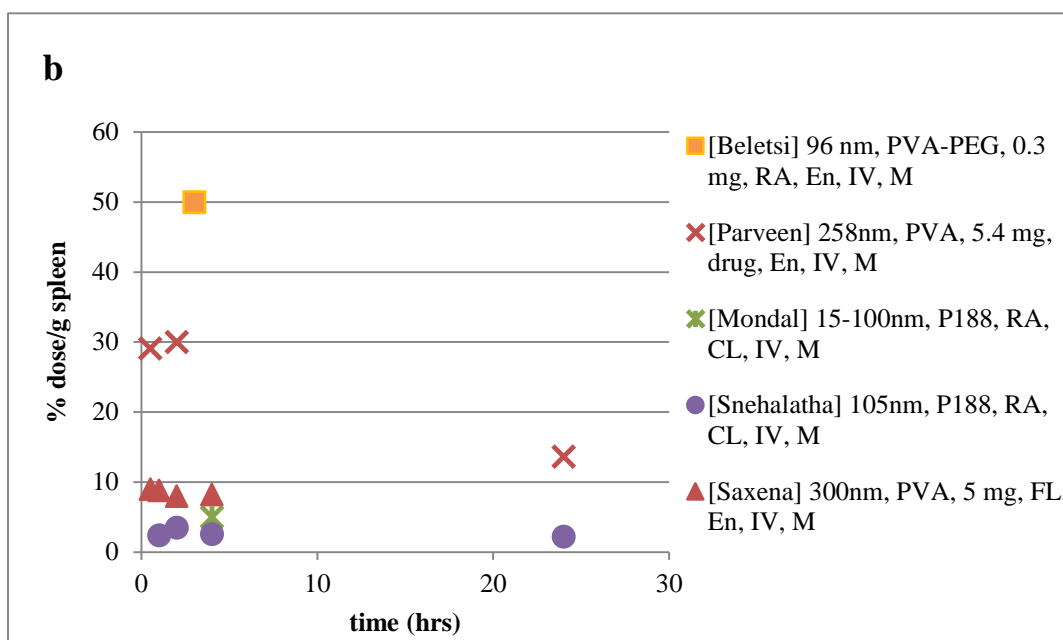


Figure 2.3. Comparative biodistribution of nanoparticles (NPs) in the spleen are shown in (a) rats and (b) mice. Data is presented as percent dose per gram of spleen with respect to time, after a single dose administered at time zero. Particle characteristics included in the legend are: [reference], nanoparticle size (mean diameter), surfactant (PVA=poly vinyl alcohol; P188=poloxamer 188, PEG=poly ethylene glycol), NP dose, detection probe (RA=radioactivity, FL=fluorescence, drug=entrapped model drug), location of detection probe (EN=entrapped, CL= covalently linked), method of NP administration (iv=intravenous delivery, o= oral delivery), and animal model (R=rat, M=mouse) (Beletsi, Panagi, and Avgoustakis, 2005; Li, et al., 2001; Mondal, et al., 2010; Parveen and Sahoo, 2011; Saxena, Sadoqi, and Shao, 2006; Snehalatha, et al., 2008; Tobio, et al., 2000; Tosi, et al., 2010; Vergoni, et al., 2009; Yin, et al., 2007).

Time profile

Of the ten NP treatments used, five showed detectable amounts in the spleen 24 hours post administration ranging from 0.15-0.4% dose/g in rats (Tobio, et al., 2000; Yin, et al., 2007) (Figure 2.3a) and 2.2-13.6% dose/g in mice (Parveen and Sahoo, 2011; Snehalatha, et al., 2008) (Figure 2.3b). For the first three hours following administration in rats, particle uptake in the spleen increased over time. For example, particles of 170 nm delivered intravenously in rats were detected at 1.2% dose/g at both 0.5 and 1 hour post administration; 1.5 hours later, a higher 2.9% dose/g spleen was present (Vergoni, et al., 2009). By the same measure, particles of 140-200 nm delivered intravenously in rats were detected at 1.7% dose/g one hour following administration, and this concentration increased to 2.8% dose/g three hours after administration (Tosi, et al., 2010) (Figure

2.3a). It was evident that particles were able to maintain consistent levels in the spleen over the first four hours following administration in mice as well (Figure 2.3b). For example, particles of 300 nm delivered intravenously in mice showed levels of 9% dose/g at 30 minutes post-delivery, and 4 hours later, 8.2% dose/g spleen was still present (Saxena, Sadoqi, and Shao, 2006) (Figure 2.3b). Following the same pattern, particles of 105 nm intravenously administered in mice showed 2.4% dose/g one hour after administration and 2.6% dose/g 4 hours after administration (Snehalatha, et al., 2008) (Figure 2.3b).

NP size

The effect of size on particle uptake in the spleen was shown in rats at three hours post administration. Particles of 200 nm delivered via i.v. administration in rats were detected at only 0.9-1.46% dose/g spleen three hours after administration (Li, et al., 2001). On the other hand, smaller particles of 140-200 nm were detected at 2.8% dose/g spleen at three hours post administration (Tosi, et al., 2010) (Figure 2.3a). In mice, particles of 96 nm were detected at a very high concentration of 50% dose/g of spleen (Beletsi, Panagi, and Avgoustakis, 2005) (Figure 2.3b). These particles were delivered intravenously and detected on the basis of entrapped radioactivity (Beletsi, Panagi, and Avgoustakis, 2005). Similarly, particles of 258 nm showed an uptake of 30% dose/g after i.v. administration of particles to mice (Parveen and Sahoo, 2011) (Figure 2.3b). Bigger particles measuring 300 nm were found at lower levels of 8-9% dose/g 1-4 hours post i.v. administration (Saxena, et. al., 2006) (Figure 2.3b). It was apparent that the smaller the size, the higher the uptake (50% for 96 nm NP, 30% for 258 nm NPs, and 9% for 300 nm NPs).

Type of indicator

Four particle systems delivered by i.v. administration in rats with entrapped indicators and similar sizes showed very consistent patterns of particle uptake. For example, particles of 170 nm with an entrapped drug reached 2.9% dose/g of spleen (Vergoni, et al., 2009), and particles of 140-200 nm with entrapped fluorescence reached 2.8% dose/g of spleen (Tosi, et al., 2010) (Figure 2.3a). Particles of 200 nm with entrapped radioactivity reached detection levels of 1.4% dose/g (Li, et al., 2001) (Figure 2.3a). Only one system used a covalently linked indicator for detection, and these particles were only reported at 24 hours (Yin, et al., 2007), showing a minimal uptake, near 0.4% dose/g, so no insights can be gained on the effect of type of probe on detection (Figure 2.3a).

The particle systems in mice showed very similar uptake patterns as seen in rats, except for their higher values. Of the particles delivered intravenously to mice, the three systems with the largest uptake were systems using entrapped indicators for detection. The highest uptake was reported at 50% dose/g for particles of 96 nm delivered i.v. (Beletsi, Panagi, and Avgoustakis, 2005) (Figure 2.3b). In contrast, two systems of particles intravenously delivered in mice showed a lower uptake when detected based on covalently linked radioactivity as indicators. Particles of 105 nm were detected at only 3.5% dose/g (Snehalatha, et al., 2008) after administration (Figure 2.3b). Similarly, particles of 15-100 nm only reached 5% dose/g on average (Mondal, et al., 2010) after administration in mice (Figure 2.3b). The difference in uptake can be attributed to the

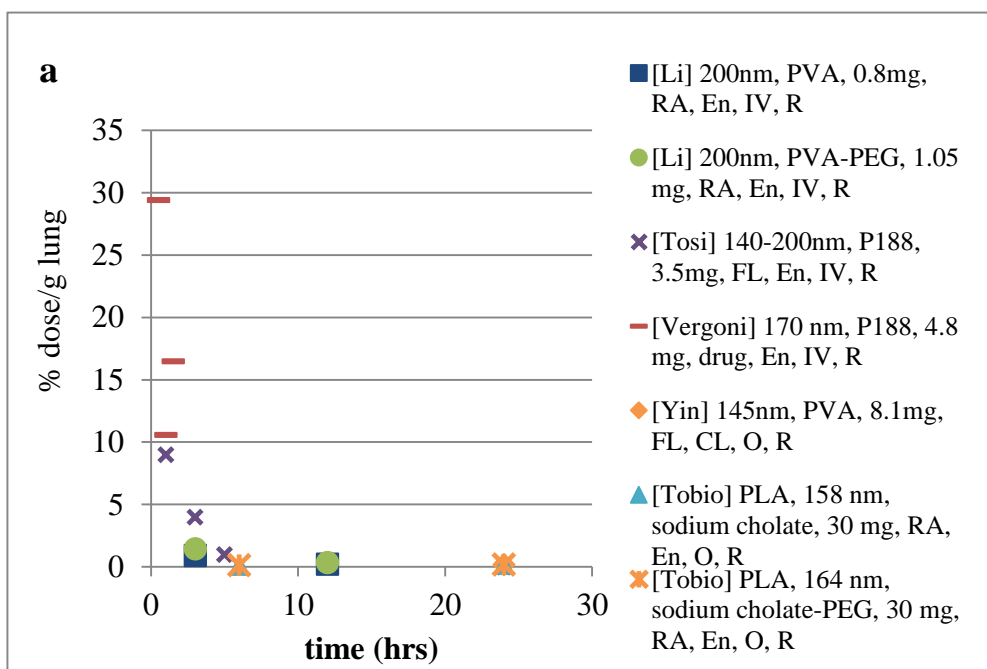
possible release of the radioactive probe when physically entrapped, leading to artificially higher uptake reported under these circumstances.

Method of delivery

Direct comparison of biodistribution of particles delivered by i.v. or oral delivery can be challenging. For example, two systems delivered orally showed little to no uptake in the spleen at 6 and 24 hours post administration in rats (Tobio et al., 2000; Yin, et al., 2007), whereas i.v. delivered particles were present at 2.9% dose/g spleen (Figure 2.3a). Perhaps orally administered particles did not make it to the tissue due to their inability to cross barriers or alternatively, the time-frame was too short for these orally delivered systems to reach the sampled tissue. If the sampling time had exceeded 24 hours, a larger presence of the particles would possibly become evident.

2.2.4 Lung

A single dose of NPs was given to mice and rats at time zero, and the particle concentration in the lungs was determined for each study for 24 hours following administration. Of these NP systems, two were administered orally (Tobio et al., 2000; Yin, et al., 2007), and eight were administered intravenously (Beletsi, Panagi, and Avgoustakis, 2005; Li, et al., 2001; Mondal, et al., 2010; Parveen and Sahoo, 2011; Saxena, Sadoqi, and Shao, 2006; Snehalatha, et al., 2008; Tosi, et al., 2010; Vergoni, et al., 2009). Concentrations of particles ranged from 0-29% dose/g in rats (Figure 2.4a) and 0.7-21.3% dose/g lung in mice (Figure 2.4b) over the 24 hours following the dose administration; at 24 hours, five of the ten NP systems confirmed undetectable levels of NPs in the lung (Figures 2.4a and 2.4b). Only NPs of 258 nm i.v. administered to mice showed a significant presence of particles at 24 hours, at 20% dose/g of tissue (Parveen and Sahoo, 2011) (Figure 2.4b).



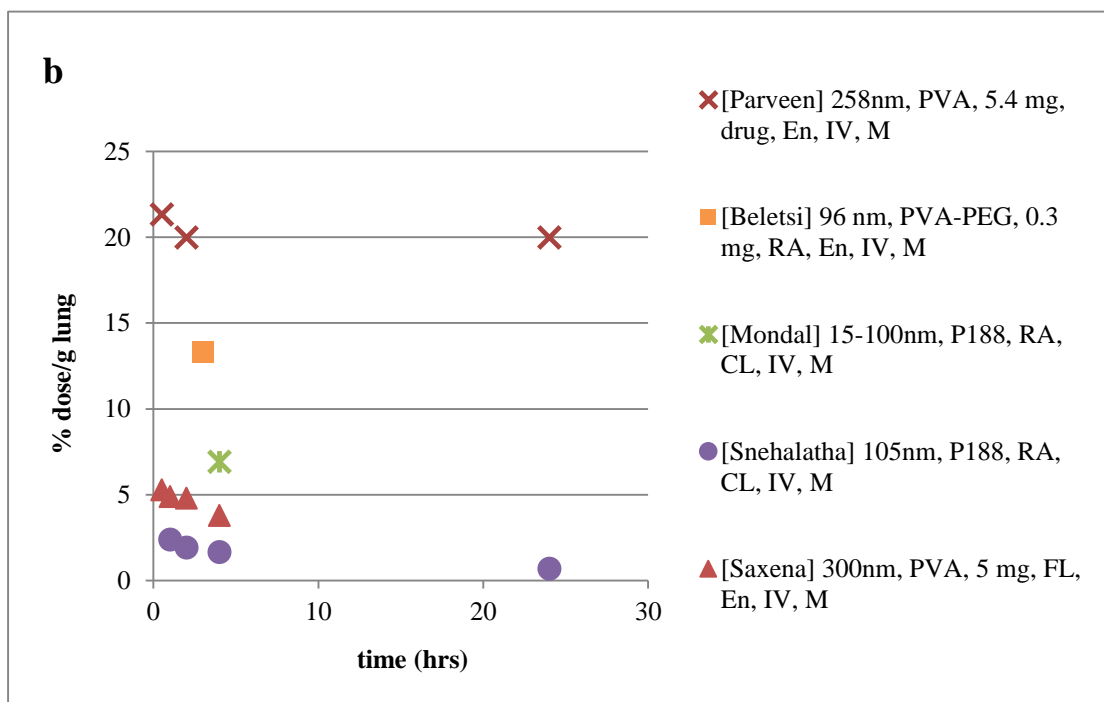


Figure 2.4. Comparative biodistribution of nanoparticles (NPs) in the lung are shown in (a) rats and (b) mice. Data is presented as percent dose per gram of lung with respect to time, after a single dose administered at time zero. Particle characteristics included in the legend are: [reference], nanoparticle size (mean diameter), surfactant (PVA=poly vinyl alcohol; P188=poloxamer 188, PEG=poly ethylene glycol), NP dose, detection probe (RA=radioactivity, FL=fluorescence, drug=entrapped model drug), location of detection probe (EN=entrapped, CL= covalently linked), method of NP administration (iv=intravenous delivery, o= oral delivery), and animal model (R=rat, M=mouse) (Beletsi, Panagi, and Avgoustakis, 2005; Li, et al., 2001; Mondal, et al., 2010; Parveen and Sahoo, 2011; Saxena, Sadoqi, and Shao, 2006; Snehalatha, et al., 2008; Tobio, et al., 2000; Tosi, et al., 2010; Vergoni, et al., 2009; Yin, et al., 2007).

Time profile

Two NP systems, both of approximately 170 nm, showed an immediate high uptake by the lungs after i.v. administration in rats. In one system, particles were detected at 29% dose/g 30 minutes after administration (Vergoni, et al., 2009). An hour later, these particles were detected at 10.6% dose/g (Vergoni, et al., 2009) (Figure 2.4a). Similarly, after one hour, the other particle system of approximately 170 nm showed an uptake of 9% dose/g in the lung (Tosi, et al., 2010) and after five hours, these particles were detected at 1% dose/g (Tosi, et al., 2010) (2.4a). Presence of both NP systems was reported one hour after administration, and at this time point, the detected amounts only differed by 1.4% dose/g (Figure 2.4a). Of the particles delivered to mice with more than one sampling time point, all particle systems decreased over time. For example, particles

of 300 nm delivered intravenously in mice were detected at 5.3% dose/g lung 0.5 hours following administration (Saxena, Sadoqi, and Shao, 2006). One half hour later, 4.9% dose/g was present, followed by 4.8% dose/g two hours post administration (Saxena, Sadoqi, and Shao, 2006) (Figure 2.4b).

Animal model

When similar systems detected with the same method were compared, rats showed smaller values of uptake compared to mice. Specifically, particles of 96 nm delivered intravenously in mice showed a presence of 13% dose/g lung 3 hours post administration (Beletsi, Panagi, and Avgoustakis, 2005), and this value was determined using entrapped radioactivity (Figure 2.4b). Particles delivered via i.v. administration in rats, on the other hand, showed only 0.9% radioactivity after three hours, and these particles were also detected using entrapped radioactivity (Li, et al., 2001) (2.4a).

Type of indicator

For NPs delivered in both mice and rats, the systems showing the highest detection were those with entrapped drugs or fluorophores for indication. For example, particles of 170 nm with entrapped drug were detected at 30% dose/g thirty minutes after i.v. delivery (Vergoni, et al., 2009). Whereas, another system of 140-200 nm particles with an entrapped fluorophore was detected at 9% dose/g one hour after i.v. delivery in rats (Tosi, et al., 2010) (Figure 2.4a). These trends were similar in mice; 258 nm particles with an entrapped drug i.v. delivered in mice showed an uptake of 21% dose/g thirty minutes after delivery (Parveen and Sahoo, 2011) (2.4b). In comparison, 96 nm particles with entrapped radioactivity were detected at 13% dose/g 3 hours after i.v. administration in mice (Beletsi, Panagi, and Avgoustakis, 2005) (2.4b). The only NPs that showed concentrations detected in the lungs greater than 8% dose/g were NPs with entrapped probes (Figure 2.4a and 2.4b).

2.2.5 Heart

After a single dose of NPs delivered to mice and rats, concentrations of particles in the heart were measured over the 24 hours following administration. Both mice and rats were given NPs, and both i.v. delivery (Mondal, et al., 2010; Parveen and Sahoo, 2011; Saxena, Sadoqi, and Shao, 2006; Snehalatha, et al., 2008; Vergoni, et al., 2009), and oral delivery (Yin, et al., 2007) were used for particle administration. Only two systems were delivered to rats (Figure 2.2.5a), and the remaining four were delivered to mice (Figure 2.5b). Five of the six NP systems were found in the heart at levels below 6% dose/g heart; a high amount (30% dose/g tissue) was detected for only one set of particles (Parveen and Sahoo, 2011) (Figure 2.5b). The particles detected at 30% dose/g were 258 nm in diameter, detected using the entrapped drug, and delivered intravenously to mice. It is important to note that this study reported in general higher uptake than the other studies consulted in this review.

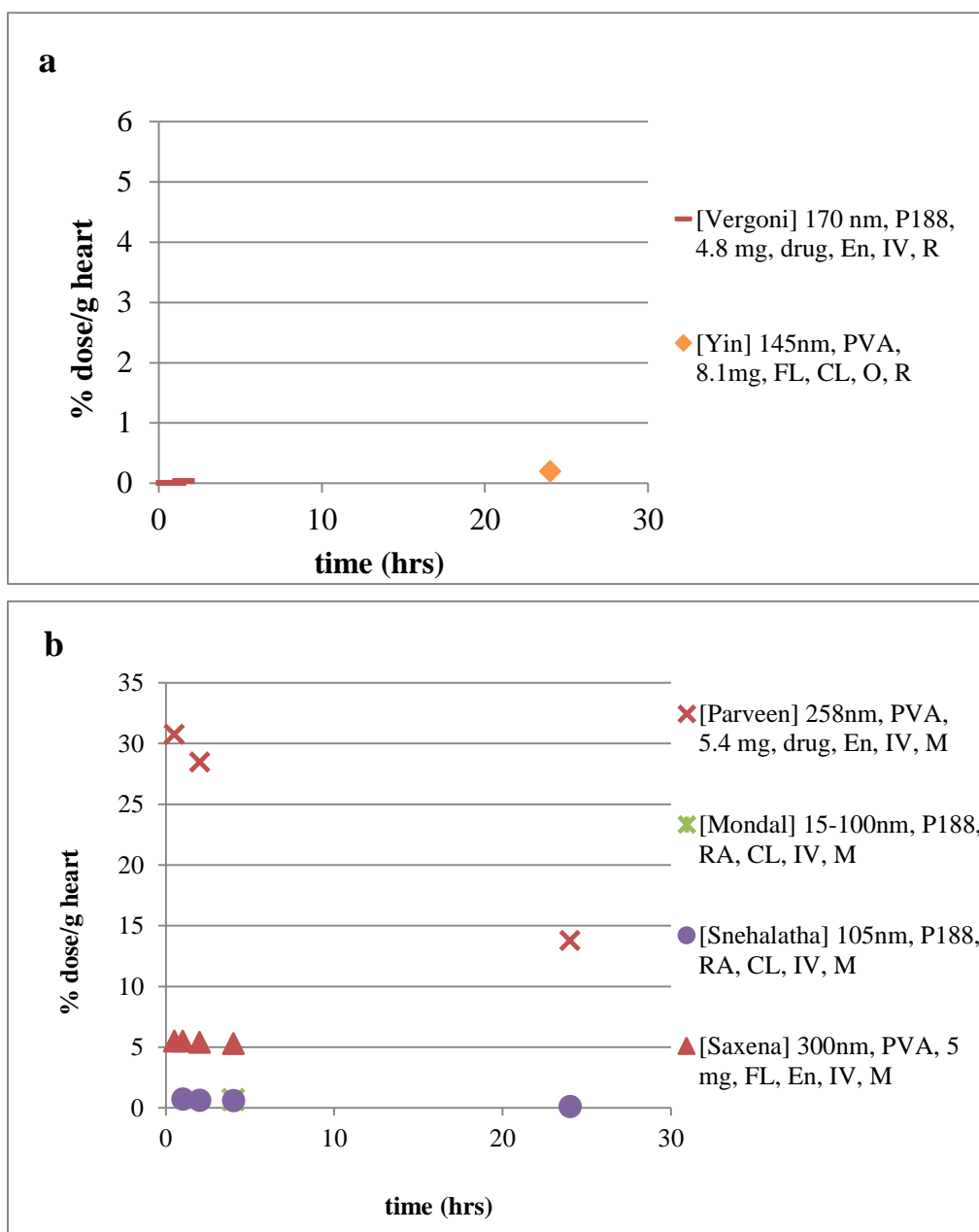


Figure 2.5. Comparative biodistribution of nanoparticles (NPs) in the heart are shown in (a) rats and (b) mice. Data is presented as percent dose per gram of heart with respect to time, after a single dose administered at time zero. Particle characteristics included in the legend are: [reference], nanoparticle size (mean diameter), surfactant (PVA=poly vinyl alcohol; P188=poloxamer 188, PEG=poly ethylene glycol), NP dose, detection probe (RA=radioactivity, FL=fluorescence, drug=entrapped model drug), location of detection probe (EN=entrapped, CL= covalently linked), method of NP administration (iv=intravenous delivery, o= oral delivery), and animal model (R=rat, M=mouse) (Mondal, et al., 2010; Parveen and Sahoo, 2011; Saxena, Sadoqi, and Shao, 2006; Snehalatha, et al., 2008; Vergoni, et al., 2009; Yin, et al., 2007).

Time profile

Of the data reported in the cited studies, the particle concentration in the heart of mice and rats approached 0% dose/g throughout the 24 hours following administration. Particles delivered to rats were detected at a maximum of 0.3% dose/g for particles of 170 nm (Vergoni, et al., 2009) and 0.2% dose/g for particles of 145 nm (Yin, et al., 2007) (Figure 2.2.5a). In mice, particles of 258 nm were delivered intravenously, and 30% dose/g was reported in the first hour. Twenty four hours later, this value decreased to 13% dose/g heart (Parveen and Sahoo, 2011) (2.5b). Four of the six particle systems reported showed little to no detection in the heart at 24 hours (Mondal, et al., 2010; Snehalatha, et al., 2008; Vergoni, et al., 2009; Yin, et al., 2007) (Figure 2.2.5a and 2.5b). It is plausible that the particles of 300 nm approached 0% dose/g 24 hours following administration in mice, but data is not reported beyond four hours post administration of these particles (Saxena, Sadoqi, and Shao, 2006) (Figure 2.5b).

Animal model

Because of the difference in organ size between mice and rats, it is expected that rats have a lower % dose/g detected in any organ. The data retrieved on heart uptake is consistent with this assumption. Particles of 170 nm delivered via i.v. administration in rats showed only 0.3% dose/g tissue in the heart for the duration of the particular analysis, 0-2 hours post administration (Vergoni, et al., 2009). In mice, particles of 300 nm were detected at 5.5% dose/g heart both 0.5 and 1 hour post administration (Saxena, Sadoqi, and Shao, 2006).

Type of indicator

An uptake of 300 nm particles, administered to mice via i.v. administration, was reported at 5.5% dose/g (Saxena, Sadoqi, and Shao, 2006) one hour post administration and detected via entrapped fluorescence (Figure 2.5b). This detected dose was much higher than that observed in mice intravenously exposed to radioactive NPs measuring 105 nm (less than 1 % dose/g) (Snehalatha, et al., 2008). The higher values detected for the entrapped fluorescent probe could be due to disassociation of the probe from the NPs. For example, the studies reporting 30% dose/g (Parveen and Sahoo, 2011) and 5.5% dose/g (Saxena, Sadoqi, and Shao, 2006) used an entrapped drug or an entrapped fluorescent probe, whereas the study that reported a low % dose/g heart (less than 1%) used a covalently linked radiolabel for detection (Mondal, et al., 2010; Snehalatha, et al., 2008) (2.5b).

2.2.6 Brain

Four NP systems were intravenously administered to rats (Tosi, et al., 2010; Vergoni, et al., 2009), and mice (Parveen and Sahoo, 2011; Snehalatha, et al., 2008), and their presence was detected in the brain. Three of the four systems showed nearly undetectable levels of particles following administration (Snehalatha, et al., 2008; Tosi, et al., 2010; Vergoni, et al., 2009). The highest of this group showed only 0.4% dose/g tissue (Tosi, et al., 2010) (Figure 2.6). NPs of 258 nm with an entrapped drug for detection showed immediate levels of 6% dose/g of brain following administration, consistent with higher values reported by this study across tissue. Even twenty-four hours

later, 4.28% dose/g was still present in the brain (Parveen and Sahoo, 2011), shown in Figure 2.6. No further insights can be drawn due to the little data reported on brain uptake of PLGA NPs.

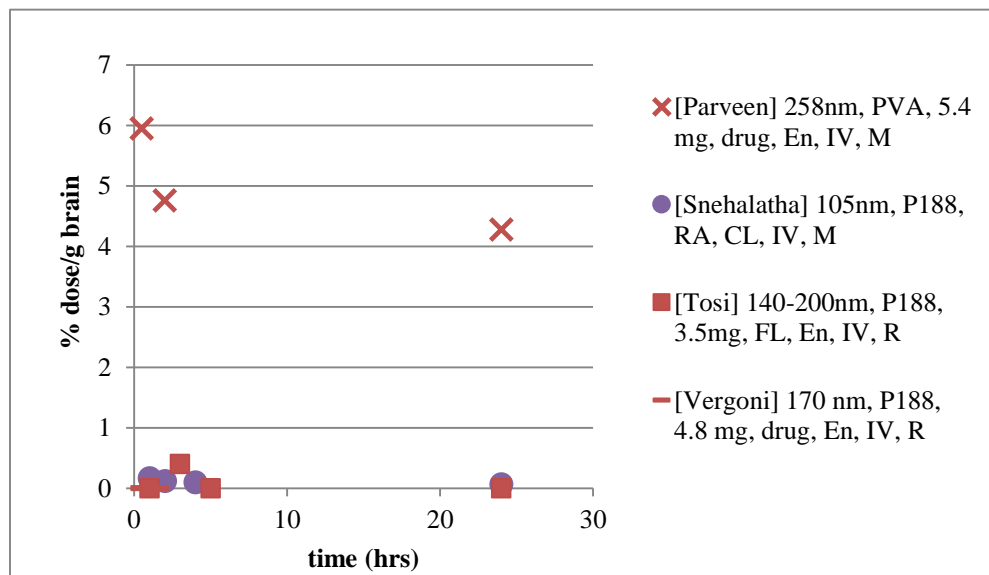


Figure 2.6. Comparative biodistribution of nanoparticles (NPs) in the brain are shown in rats and mice. Data is presented as percent dose per gram of brain with respect to time, after a single dose administered at time zero. Particle characteristics included in the legend are: [reference], nanoparticle size (mean diameter), surfactant (PVA=poly vinyl alcohol; P188=poloxamer 188, PEG=poly ethylene glycol), NP dose, detection probe (RA=radioactivity, FL=fluorescence, drug=entrapped model drug), location of detection probe (EN=entrapped, CL= covalently linked), method of NP administration (iv=intravenous delivery, o= oral delivery), and animal model (R=rat, M=mouse) (Parveen and Sahoo, 2011; Saxena, Sadoqi, and Shao, 2006; Snehalatha, et al., 2008; Tosi, et al., 2010; Vergoni, et al., 2009).

2.3 Discussion

The PLGA NPs featured in this review ranged from 15 nm-300 nm and were delivered in mice or rats, with covalently linked or entrapped indicators for detection. Some particle systems utilized radioactivity while others used fluorescence or an active drug for detection. Although biodistribution of nanoparticles is directly affected by the NP system properties, the fate of nanoparticles *in vivo* is a result of the synergistic effects between each of these NP properties. For example, route of administration and particle size are both directly related to rate of degradation of the NPs, which then affects biodistribution and proper detection of the NPs. On the other hand, increasing sizes can allude to slower rates of degradation. By the same token, increasing hydrophilicity of the NPs accomplished by addition of various surfactants results in different uptake rates and biodistribution profiles. In addition to affecting biodistribution, degradation of particles also influences the fate of the associated detection probes. The more deterioration experienced by NPs, the less likely it is that nanoparticles will be associated with their

detection probe, whether it is physically entrapped or covalently linked. This phenomenon would result in misleading data regarding particle biodistribution.

In order to compare particle behavior *in vivo*, it is important to remember that each particle system had a set of characteristics that were not shared with every other particle system featured in this review. Differences in animal model and delivery method had the largest influence on particle behavior, but differences in method of detection (location of probe), size, surface modification, surfactant, and dose may have also affected biodistribution of particles.

Although inconsistencies exist in the particle characteristics among the studies, patterns of biodistribution were identifiable. These patterns are important because they give researchers a sense of expectation when designing PLGA NPs for drug delivery in mice and rats. When PLGA particles of 140-200 nm were delivered intravenously and orally to rats, uptake between 0-4% dose/g liver was detected (Figure 2.1a). On the other hand, PLGA particles of 15-300 nm delivered intravenously to mice were detected between 5 and 40% dose/g liver over a 24 hour time period following administration, depending on their physical characteristics (Figure 2.1b). Similarly, kidney uptake in rats showed between 0 and 4% dose/g of particles in the first four hours, but only small amounts of particles were detected at 24 hours (Figure 2.2a). In mice, particles of 15-300 nm were found mostly between 2-8% dose/g kidney. Some particles were still present in the kidney up to 2% and 15% dose/g tissue in mice 24 hours after a single dose administration (Figure 2.2b). PLGA NPs of 140-200 nm delivered both orally and intravenously to rats were detected at values between 1 and 3% dose/g spleen in the first two hours following administration (Figure 2.3a). Mice showed a wider range of values for spleen uptake of particles; 2.5-9% dose/g tissue was identified in mice after i.v. delivery of particles ranging from 15-300 nm (Figure 2.3b). The lungs showed much less of a trend in uptake of PLGA NPs than other organs analyzed. In rats, uptake values ranged from 9-29% dose/g lungs after delivery in the first two hours (Figure 2.4a). In mice, 2.4-21% dose/g tissue was detected in the first two hours (Figure 2.4b). The heart and brain showed very little uptake of particles. For both organs in rats and mice, all particle systems with two exceptions (Parveen and Sahoo, 2011) (Saxena, Sadoqi, and Shao, 2006) were detected between 0-1% dose/g across all time points.

Analysis of biodistribution of polymeric NPs over time is critically important. Polymeric NPs are designed to be biocompatible and biodegradable; data showing clearing of these NP systems from tissue over time would support this concept. The time it takes for PLGA NPs to clear the body is different depending on the particle properties. From the literature consulted for this review, it was apparent that 24 hours after administration (oral or i.v.), the amounts available in tissue is minimal for all PLGA NPs studied, of different sizes (15-300 nm), surfactant used (PVA, P188, PEG), NP dose, detection probe, location of detection probe, and animal model.

For example, in the liver, five of the seven reported particle systems delivered to rats were detected at levels under 1.1% dose/g 24 hours following administration (Figure 2.1a). Similarly, four of the five NP treatments delivered to rats showed less than 1.5% dose/g in the kidney at 24 hours (Figure 2.2a). Similar trends were seen in mice. Reported values for each mouse organ decreased over time towards 0% dose/g; but few studies actually reported a particle concentration at 24 hours in mice, most focusing on the first four hours post administration

The data reflected in the reviewed studies reinforced the presumption that size affects NP uptake and biodistribution. According to Parag Aggarwal, et. al, (2009) biological responses upon NP administration tend to depend more on surface area than on mass. The smaller the particle, the larger is the surface area to volume ratio. This larger surface area creates more room for protein binding of the particles, creating a protein “corona”. Specific components of this corona, called opsonins, perhaps enhance uptake of the NP by the cells of the reticulo endothelial system (RES). These RES cells are highly concentrated in the liver and spleen; and the data has shown higher uptake of smaller NPs in both of these organs (Figure 2.1a, Figure 2.1b, Figure 2.3a, Figure 2.3b). In addition, it was reported that smaller NPs can penetrate through the fenestrae in the endothelial lining of the liver which has a mean diameter of 100 nm (Beletsi, Panagi, and Avgoustakis, 2005), and this concept was reinforced by the reviewed data.

The time profile was different across animal models. Although mice and rats have similar anatomies, their relative organ sizes are not comparable (Table 2.2). Therefore, higher levels of NPs might be detected in mice more quickly than in rats, but when divided by the organ weight for the same initial dose, the % dose/g tissue is smaller in rats than mice. Similarly, the rate at which certain organs show high levels of particles varies on the particular organ.

The time points reported in the literature and included in this review were limited. Some publications only showed data from tissue collection once after administration of the particles. Others may have reported several different time points after administration, but unless each data set used the same time points, comparing data across studies is impossible without taking this difference into account.

Detection of particles in the various organs depends on how long it takes the particles to travel in the blood to the particular organ. When an increase in NP concentration is seen over time in organs such as the liver or spleen, it can be attributed to a longer blood residence time (Mondal, et al., 2010). This was evident in the spleen, which is part of the RES, in both rats and mice. For example, particles of 140-200 nm were detected at 1.7% dose/g after 1 hour following administration in rats, but at 3 hours post administration, an increased 2.8% dose/g was detected (Tosi, et al., 2010) (Figure 2.3a). Similar results were seen in the spleen for the first two hours following i.v. injection in mice (Parveen and Sahoo, 2011; Snehalatha, et al., 2008) (Figure 2.3b). This increase of uptake in the spleen was perhaps due the reduced NP uptake by the liver (Beletsi et al. 2005).

Each particle in this review utilized an indicator that was either physically entrapped in the particle or was covalently linked to the particle. The behavior of the radioactive or fluorescent probes *in vivo* was highly dependent on the location of probe association with the NP (covalently linked vs. entrapped). For example, particles of 300 nm loaded with ICG, used for detection, released 78% of the entrapped ICG in sink conditions using phosphate buffered saline at pH 7.4 in just 8 hours (Saxena, Sadoqi, and Shao, 2006). Similarly, in particles of 170 nm delivered intravenously in rats, the entrapped fluorophore, Rh-123, was used for detection. The association of the Rh-123 with the NPs was proven under physiological conditions for a time shorter than 2 h. By 24 hours, 35% of the entrapped Rh-123 was released from the NPs (Vergoni, et al., 2009). It is possible that at times that exceed 2 h, fluorophores like Rh-123 and ICG may leak from the particles and their detection may not be associated with NP presence.

It was evident in this review that particles using entrapped probes showed higher concentrations in all organs studied (Beletsi, Panagi, and Avgoustakis, 2005; Parveen and Sahoo, 2011; Tosi, et al., 2010; Vergoni, et al., 2009). On the other hand, particles using covalently linked probes showed much lower concentrations in tissues (Mondal, et al., 2010; Snehalatha, et al., 2008). These seemingly lower concentrations may be the most accurate of the data sets. According to Yin, et al. (2007), in order to complete an *in vivo* study involving biodistribution, stable binding of fluorescent marker to a polymer as well as retainment of fluorescent intensity during assay are required. When 145 nm PLGA NPs were synthesized with a covalently linked indicator, only 0.7-0.9% of the marker was quenched or released from NPs after 72 hours of artificial gastric and intestinal incubation. Because the indicator stayed intact, false results would only result from degradation of the polymer, not diffusion of the marker from inside the polymer.

The fates of orally ingested particles and intravenously injected particles are drastically different. Biodistribution is one of four processes a drug follows after oral delivery, and distribution relies on the first and preceding process, absorption. Absorption describes the passage of drug molecules from the location of administration into the circulation (Brenner & Stevens, 2009). In oral delivery, NPs must first be absorbed through a layer of epithelial cells in the gut that have tight junctions, creating a barrier of absorption. In order for an orally delivered NP to reach circulation for further distribution, it must cross these biological barriers. NPs administered intravenously bypass these biological barriers and enter directly into circulation. It is therefore understood that i.v. delivered NPs have 100% bioavailability (Brenner & Stevens, 2009), meaning more of the administered dose is available for distribution at a much faster rate. The higher percentage of i.v. administered NPs in various tissues when compared to the orally delivered NPs was expected. Results reported for orally delivered nanoparticles indicated that small amounts of particles were absorbed through the gut into the circulatory system.

An alternative explanation of the low dose observed over 24 hours in different tissues of animals treated orally with PLGA NPs can be the relatively short sampling time. One study featuring oral delivery of PLGA NPs but focused only on bioavailability of the active drug in the blood indicated that the maximum concentration of 150 nm PLGA particles in the blood occurred 12-32 hours post oral administration in rats (Mittal, et al., 2007). In contrast, particles of 200 nm delivered intravenously in rats showed a maximum concentration 15 minutes after injection (Li, et al., 2001). It is hence possible that at longer times, concentrations of orally delivered PLGA NPs may reach higher values than those observed in the sampled studies, limited to 24 hours.

It is important to note that data is limited on oral delivery of PLGA NPs, and a definite gap is present in this area. Only two studies using oral delivery were featured in this review, and patterns shown on biodistribution of orally delivered PLGA NPs are inconclusive based solely on these two references.

2.4 Conclusion

The goal of compiling available data on PLGA NP biodistribution and quantitatively presenting NP presence in major tissue over time was achieved in this review. The data was converted and combined to provide a uniform, comprehensive analysis of published data. The clarity of the presented data allowed for several trends involving PLGA biodistribution in mice and rats to become evident. A range of concentrations of NPs was identified for each organ; the liver, lung, kidney, and spleen

showed the highest uptake, while the brain showed essentially no uptake. The NP uptake was dependent on many characteristics including type of animal, method of delivery, size of the NP, and type of indicator used in NP detection. Mice showed higher concentrations in tissues than rats, which is expected due to their smaller organs. Similarly, i.v. delivery showed a higher uptake than oral delivery, but little data on oral delivery of PLGA NPs exists to reinforce this observation. Smaller sizes were detected in higher concentrations in the liver, kidney, and spleen. Finally, physically entrapped indicators were detected in higher concentrations, perhaps due to disassociation of the indicator probe from the NP, which would cause these values to be misleading. Covalently linked probes showed stronger association to the NP *in vitro*, and they showed smaller concentration values *in vivo*. These smaller values are plausibly more accurate than the larger ones because they represent the location of the NP, not the location of a leaked probe. More data is needed to determine trends of oral delivery of PLGA NPs as well as biodistribution profiles of particles 24 hours following administration. Despite these gaps in data, this review provides researchers a more accurate sense of PLGA NP biodistribution and NP behavior *in vivo*. The scope of the presented information creates a more solid foundation for research on improvements in drug delivery and drug efficacy that rely on nanotechnology such as PLGA NPs.

Chapter 3 Bioavailability of Alpha-tocopherol Entrapped in Poly (lactide-co-glycolide) (PLGA) and PLGA-Chitosan Nanoparticles

3.1 Introduction

Alpha-tocopherol (α T), a free radical chain-breaking antioxidant, is the most bioactive form of vitamin E, and when consumed by humans, has shown to provide numerous health benefits (Song, et al., 2009). This lipophilic antioxidant faces challenges common to other orally-delivered lipophilic antioxidants including poor solubility in water, oxidative instability when exposed to heat, light, and oxygen, chemical and enzymatic instability in the GI tract, and low mucosal permeability (Cohn, 1997; Murugesu et al., 2011; Brenner & Stevens, 2010). In addition, the absorption, transport, and distribution of α T is linked to dietary fat (Lodge, 2005). Because of the connection between dietary fat and α T absorption, the bioavailability of α T is highly variable. Bioavailability, as defined by the FDA, is the rate and extent to which the active drug ingredient or therapeutic moiety is absorbed and becomes available at the site of action (Cohn, 1997).

Nanoparticles, as alternative delivery systems, have a plethora of advantages over other delivery systems including the ability to deliver insoluble drugs, the ability to target drugs within the body, and the ability to support transcytosis of a drug across the tight intestinal barrier for improved bioavailability. In addition, nanoparticles are able to protect the drug from gastro-intestinal degradation, prolong systemic circulation, reduce fed/fasted variable absorption, and control the release of the drug (Grama et al., 2011). It is therefore expected that with all the aforementioned advantages of nanodelivery systems, bioavailability of orally-delivered drugs in nanoform will be improved. Several studies indicated that indeed, poly (lactic-co-glycolic) acid (PLGA) NPs have improved bioavailability of drugs compared to their free form, such as cyclosporine (119% of free form) (Italia et al., 2007), estradiol (1014%) (Mittal et al., 2007), doxorubicin (363%) (Grama et al., 2011), amphotericin B (793%) (Grama et al., 2011), and curcumin (2583%) (Grama et al., 2011), (2200%) (Tsai, et al., 2011), (1560%) (Khalil et al., 2012).

In order to address the variable, and often low, bioavailability of α T, researchers have attempted different ways to improve uptake of this bioactive by entrapping it into delivery systems. In general, the area under the curve (AUC) of α T increased for all systems studied. When the AUC of the α T delivered to rats in free and nano-emulsion systems were compared, the nano-emulsion delivered α T showed a 143% increase in bioavailability compared to the control (free) form (Hatanaka et al., 2010). The AUC of α T was 18% higher compared to α T delivered in free form when entrapped in a calcium-pectinate microparticle system and delivered to rats (Song, 2009). A two-fold increase in α T bioavailability was achieved in humans when delivered as Gelucire 44/14 product (Barker, 2003).

Two mechanisms are proposed for improved bioavailability of nanodelivered drugs. Either the drug is transported with the nanoparticles as they are transcytosed, or

the particles release the load in a controlled manner in the intestine, where it is efficiently absorbed. It is suggested that orally administered nanoparticles travel through the GI tract where they are absorbed by endocytosis, or by lymphoid uptake, in the “M-cells” in the Peyer’s patches (Mittal et al., 2007). Alternatively, the nanoparticles may adhere to the M-cells and release only the entrapped drug into the cell. Mucoadhesive nanoparticles are believed to improve bioavailability of poorly absorbed drugs because of the strong attraction of the particles to the negatively charged mucosa of the intestine responsible for a longer residence time in the intestine (plapied et al., 2011). Chitosan can be used to confer a positive charge to PLGA NPS when deposited on the surface of the particles via electrostatic interaction, to form a mucoadhesive PLGA-Chitosan (PLGA-Chi) NP.

It is hypothesized that PLGA and PLGA-Chi nanoparticles will improve the bioavailability of nanoparticle-entrapped α T when compared to free α T, and further, it is hypothesized that the mucoadhesive properties of PLGA-Chi will increase the bioavailability of entrapped α T when compared to α T delivered in PLGA NPs. To test the hypotheses, PLGA and PLGA-Chi nanoparticles were orally administered to rats, and the pharmacokinetic profiles of the NP-delivered treatment were compared to that of the control, or free α T. To better explain the observed pharmacokinetic profile of the NP-delivered α T, the release kinetics of α T from both NP systems were studied. In addition, the physical stability of the NPs and the chemical stability of the entrapped α T were examined.

3.2 Materials

Poly (D,L-lactide-co-glycolide) (50:50) with a molecular weight of 30,000-60,000 Da, Polyvinyl alcohol (PVA) (31,000-50000 Da), (\pm)- α -tocopherol (96%), and D-(+)-Trehalose dehydrate $\geq 99\%$ were purchased from Sigma Aldrich (MO, USA). Chitosan with a molecular weight of 100-300 kDa was purchased from Acros Organics, and ethyl acetate was obtained from Macron Chemicals. Nanopure water was obtained with Nanopure Diamond (Barnstead international, IA, USA). Acetonitrile and methanol, HPLC grade, were obtained from EMD Chemicals (USA). Acetic acid was purchased from Fischer Scientific (New Jersey, USA). Gastric media was made up of nanopure water, pepsin from porcine gastric mucosa (Sigma Aldrich), hydrochloric acid purchased from Fisher Scientific, and sodium chloride also purchased from Fisher Scientific. The intestinal media is composed of nanopure water, pancreatin purchased from Sigma Aldrich, and sodium hydroxide and potassium hydrogen phosphate both obtained from Fisher Scientific. Pasteur pipettes and heparin tubes were both purchased from Fisher Scientific. Male F344 rats were purchased from Harlan (Indianapolis, IN, USA). Bio-Serv (Frenchtown, NJ) provided both rat feed and corn oil stripped of tocopherols.

3.3 Methods

3.3.1 Nanoparticle Synthesis

PLGA and PLGA-Chi particles with entrapped α T were synthesized using emulsion evaporation method modified from Zigoneanu et al. (2008). First, the organic phase was composed of 2.5 w/v% PLGA and α T at a 10 w/w% loading relative to PLGA mass dissolved in ethyl acetate. The aqueous phase was formed with 2% polyvinyl alcohol (PVA) dissolved in ethyl acetate-saturated nanopure water. The organic phase was then slowly added to the aqueous phase at an oil to water ratio of 1:5 under continuous mixing. After the initial emulsification, the emulsion was subjected to three rounds of microfluidization at 30,000 psi to further reduce the size of the droplets. Once the emulsion was completely formed, the ethyl acetate was evaporated under vacuum in a rotovapor (Buchi R-124, Buchi Analytical Inc., DE, USA). Following complete evaporation of ethyl acetate, an aliquot of the sample was used to form PLGA-Chi particles. A 0.01 w/v% chitosan solution was formed using nanopure water spiked with acetic acid, creating an acidic environment for proper chitosan solubility. The chitosan solution was added to the separated nanoparticle sample at a chitosan concentration of 10 w/w% relative to PLGA and mixed thoroughly using a magnetic spin bar. The final PLGA and PLGA-Chi nanoparticle suspensions were washed by dialysis with a 100 kD MWCO membrane suspended in 1.5 L water to remove the PVA, with water changes every 8 hours for 72 hours. Finally, particles were lyophilized for 48 hours in the presence of trehalose as a cryoprotectant at a trehalose to particle ratio of 1:1.

3.3.2 Entrapment Efficiency

Entrapment efficiency of lyophilized nanoparticles was determined by dissolving the powder (trehalose and particles) in 95:5 (v/v%) acetonitrile:water at a concentration of 0.2 mg mL⁻¹. The solution was sonicated for 1 minute before incubation for two hours at ambient temperature. Following incubation, the sample was centrifuged at 30,000 rpm for 15 minutes in an Allegra 64R centrifuge (Beckman Coulter, Fullerton, CA, USA), then filtered with a 0.2 μ m PVDF syringe filter. An Agilent 1200 HPLC (Santa Clara, CA, USA) with a binary pump, autosampler, and reverse-phase C18 Xorbax XDB column was employed for fluorescent detection of α T at an excitation and emission of 290 nm and 330 nm, respectively. The mobile phase involved 1 mL min⁻¹ gradient flow of 10% water and 90% methanol, increasing to 100% methanol over 8 minutes. The total analysis time was 21 minutes per injection. 25 μ L of the filtered sample was injected by the autosampler, and the area under the curve produced by the fluorescence detector was automatically integrated by Agilent Chemstation software.

A calibration curve with concentrations ranging from 6 – 0.1 μ g/ml α T in 95:5 acetonitrile:water was produced to determine sample concentration from area under the curve. All linear curves used in this study had a correlation coefficient of at least > 0.99, and inter and intra-assay variabilities were determined by quantifying n=3 replicates at

five different concentrations of α T. Entrapment efficiency was determined by dividing the mass of α T per mg of powder by the theoretical mass of α T/mg powder.

3.3.3 Nanoparticle Morphology, Size, PDI, Zeta Potential

Particle morphology was identified by transmission electron microscopy (TEM) using a JEOL JEM-1400 (JEOL USA Inc., Peabody, MA) system. Lyophilized nanoparticles were resuspended in DI water, and one droplet of both PLGA and PLGA-Chi NPs in suspension was placed on a copper grid of 400 mesh with carbon film. Uranyl acetate (2%) was used as a stain, and the sample was dried before analysis. Size, polydispersity index (PDI), and zeta potential were measured by dynamic light scattering (DLS) using a Malvern Zetasizer Nano ZS (Malvern Instruments, Inc., MA, USA). For analysis, freeze-dried NPs were resuspended in deionized water at a concentration of 0.1 mg ml⁻¹. One mL of the particle suspension was measured in clear disposable zeta cells at 25°C. The refraction index and viscosity were set equal to that specific to DI water. The mean values of size, PDI, and zeta potential were determined using a mono-modal distribution.

3.3.4 Nanoparticle Physical Stability

The pH stability of the PLGA and PLGA-Chi nanoparticles was determined using the Malvern Zetasizer Nano ZS. Particles were suspended in nanopure water that was titrated from pH 2.5-9 in increments of 0.5 using dilute HCL and NaOH solutions (Murugesu et al., 2011). The pH progression was designed to mimic pH change during GI transit. Size and zeta potential were determined at each increment of pH 0.5, and one measurement per 0.5 pH increment was taken for both PLGA and PLGA/Chi NPs.

3.3.5 Alpha-tocopherol Chemical Stability

The chemical stability of α T was determined by exposing both PLGA and PLGA-Chi NPs with entrapped α T to physiological conditions and measuring the remaining α T present in the media. Specifically, the NPs were suspended at 3 mg NPs/ml in simulated gastric and intestinal media, and the suspensions were kept at 37 °C and 100 rpm. The simulated gastric media consisted of 3.2 mg/ml pepsin, 0.03M NaCl, and 7ml HCL/l media, all dissolved in nanopure water at a pH of 1.2. The intestinal media contained 10 μ g/ml pancreatin, 0.05M KH_2PO_4 , and 0.896 g NaOH/l media, all dissolved in nanopure water, at a pH of 6.8. At various time intervals from 0-3 hours (gastric) and 0-72 hours (intestinal), a sample of the suspension was centrifuged for 90 minutes at 30,000 rpm, and the α T was extracted from both the pellet (NPs) and the supernatant (released α T). The amount of α T was determined using the HPLC method described in the entrapment efficiency section. The sum of the two quantities revealed the total amount of α T present, and this number was compared to the total amount of α T determined by the entrapment efficiency at time zero.

3.3.6 Nanoparticle Release Kinetics

In vitro release profiles of α T from PLGA and PLGA-Chi nanoparticles were determined under simulated gastric and intestinal environments outlined in section 2.3.5 (Chemical Stability). Following preparation of the gastric and intestinal environments, PLGA and PLGA-Chi particles were suspended in the gastric or intestinal solution at a concentration of 3 mg/ml and placed in an incubator at 37°C and 100 rpm. One ml samples were collected in triplicate at multiple time points over the course of the experiment, 3 h under gastric and 72 h under intestinal conditions. Samples were centrifuged at 30,000 rpm for 90 minutes to separate the particles. Following particle centrifugation, α T was extracted from the collected particles as previously described for entrapment efficiency measurement.

3.3.7 Nanoparticle Delivery Media Preparation

In order to confirm that PLGA and PLGA-Chi NPs effectively increased bioavailability of entrapped α T when compared to free α T, it was critical to deliver all treatments and control in the same media. Since bioavailability of α T is dependent on the presence of dietary lipids, a special delivery system was made, keeping the amount of lipids constant. The delivery vehicle consisted of a flour-in-water slurry, made up of 300 mg/ml refined flour, which was combined with corn oil stripped of α T (Bio-Serv, Frenchtown, NJ) at a ratio of 30:70. The nanoparticles or free α T was dissolved in this slurry prior to delivery. Each of the treatments included 1.5 mg α T (entrapped in NPs or in free form) delivered in the slurry in a 1 ml dose.

3.3.8 Experimental Animals

All experimental protocols involving animals were approved by the Louisiana State University Institutional Animal Care and Use Committee (Baton Rouge, LA). Male F344 rats (Harlan Laboratories, Indianapolis, IN) weighing 240 ± 6 g were housed two per cage and were acclimated for one week with access to food and water *ad libitum*. During the last four days of the acclimation period and duration of the study, the rats were fed AIN-93G rodent diet (Bio-Serv, Frenchtown, NJ) which was stripped of all tocopherols. The rats were fasted 12 hours prior to treatment with free access to water, and n=6 rats were gavaged at time 0 for both treatments and control doses. After gavage, the tocopherol-free feed was replaced, and the rats were allowed unlimited access. During blood collection, the rats were temporarily anesthetized with isoflurane. Blood was collected via the retro-orbital plexus over 72 hours after gavage, and the collection time points included 0, 2, 4, 8, 12, 24, 36, 48, and 72 hrs. The collected blood was transferred to lithium heparin tubes to prevent clotting, and the plasma was separated from the blood immediately after by centrifugation at 6,000 rpm for 8 minutes at 20 °C.

3.3.9 Alpha-tocopherol Plasma Concentration Measurement

The collected plasma was stored at -80 °C until processing and analysis. In order to determine the α T concentration in the plasma, 25 μ l of the plasma was thawed and spiked with delta-tocopherol (dT) as an internal standard (IS). The final IS concentration was 0.1 μ g/ml. Acetonitrile was added to the spiked plasma to precipitate the proteins at a 95:5 acetonitrile:plasma ratio. After, the mixture was sonicated for 1 minute in 1.5 ml eppendorf tubes and allowed to sit undisturbed for 2.5 hours. The samples were then centrifuged at 30,000 rpm for 15, and the supernatant was filtered through a 0.2 μ m PVDF syringe filter before being subjected to HPLC-MS analysis, as follows.

Electrospray analysis was completed using an Agilent 1200 liquid chromatograph with autosampler, in sequence with an Agilent 6210 mass spectrometer. The 6210 is an ESI – TOF (ElectroSpray Ionization – Time Of Flight) instrument. Separation was accomplished using a Zorbax SB-C18 column (2.1 x 30mm, 3.5-Micron) (Agilent Technologies, Santa Clara, CA). The injection volume was 10 μ l, with a mobile phase consisting of A: water with 0.1% formic acid and B: methanol with 0.1% formic acid at a flow rate of 0.2 ml/min. The gradient was as follows: 90% methanol and 10% water at time 0, then methanol increased to 100% after 8 minutes. This stayed constant until the run is over at 21 minutes after injection.

For purposes of data analysis, the following ions were extracted from the total chromatogram: 429-431 m/z for α T and 402-403 m/z for dT. Extracting these ions resulted in peaks that were integrated using the areas for analysis. A ratio was calculated with the area of the α T divided by the area of the dT using MassHunter.

The sample data were compared with a calibration curve prepared by spiking blank plasma samples with various amounts of a stock solution of α T and a constant concentration of 0.1 μ g/ml (final) δ T internal standard (IS). The following concentrations made up the curve: 0.05, 0.1, 0.5, 1.0, and 2.0 μ g α T/ml. All linear curves used in this study had a correlation coefficient of at least > 0.99. Both inter and intra-assay variabilities were determined by quantifying n=3 replicates at five different concentrations of α T using the HPLC-MS method described for sample processing.

3.3.10 Pharmacokinetic Analysis

The pharmacokinetic parameters were calculated using NCSS 9, version 9.0.7 (Kaysville, UT, USA). The trapezoidal rule was employed to determine the AUC for oral administration of both treatments and controls. The area under the concentration-time curve (AUC) is a means to quantify the total amount of drug (α T) that reaches systemic circulation. The relative bioavailability used in this study (F) is defined as the AUC of the drug orally delivered by a specific system divided by the AUC of the drug orally delivered in free form. C_{\max} represents the maximum concentration of the drug detected in the plasma, and T_{\max} is the time at which this occurs.

3.3.11 Statistical Analysis

The statistical significance of the data was determined using SAS® (SAS Institute Inc., Cary, NC, USA). A mixed models analysis of variance with random mixed effects procedure was used to estimate the significance of the all data, and difference between the means was presumed significant if the *p*-value was less than or equal to 0.05.

3.4 Results

3.4.1 Entrapment efficiency

The entrapment efficiency was determined by comparing the amount of α T present in the nanoparticles to the theoretical amount of α T used in the synthesis of the particles. The amount of α T measured in the PLGA NPs was 25.12 ± 2.6 μ g/mg NPs, and the amount measured in the PLGA-Chi NPs totaled 19.49 ± 0.38 μ g/mg NPs. According to the theoretical values, these measurements confirm a $95.4 \pm 9.85\%$ entrapment efficiency in the PLGA NPs and a $77.95 \pm 1.51\%$ entrapment efficiency in the PLGA-Chi NPs.

3.4.2 Nanoparticle morphology, size, polydispersity, and zeta potential

The PLGA and PLGA-Chi NPs showed a spherical morphology when measured by TEM (Figure 3.1). According to DLS analysis, the PLGA and PLGA-Chi NPs had an average diameter of 97.87 ± 2.63 nm and 134.1 ± 2.05 nm and a PDI of 0.156 and 0.298, respectively. The zeta potential of the PLGA NPs was -36.2 ± 1.31 mV, while the zeta potential of the PLGA-Chi NPs was 38.0 ± 2.90 mV.

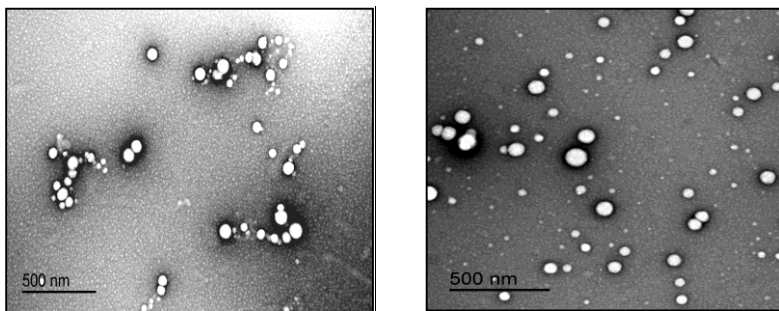


Figure 3.1. PLGA NPs (L) and PLGA-Chi NPs (R) are visibly spherical in shape when observed by TEM.

Although there are numerous limitations in fully simulating physiological environments *in vitro*, useful information can be extracted by exposing nanoparticles to conditions that mimic the GI environment. A battery of tests was applied to learn if the nanoparticles maintained their nanometer-scale size, if the bioactive was protected by the nanodelivery systems during the GI transition, and how much α T was released under these conditions. The information acquired was important in trying to decide whether the α T detected in plasma was shuttled across the intestine by the PLGA or PLGA-Chi NPs,

or if the particles adhered to the intestinal mucosa and only released α T was absorbed and introduced into circulation, free of the particle.

3.4.3 Nanoparticle Physical Stability

The results for pH stability of both particle systems showed very favorable results. Throughout the pH titration, the average diameter of the PLGA NPs only changed 4 nm, from 110 nm-114 nm (Figure 3.2). Even with the neutral zeta potential shown in Figure 3.2, the size remained constant. This data builds confidence in the size stability of the PLGA NPs *in vivo*.

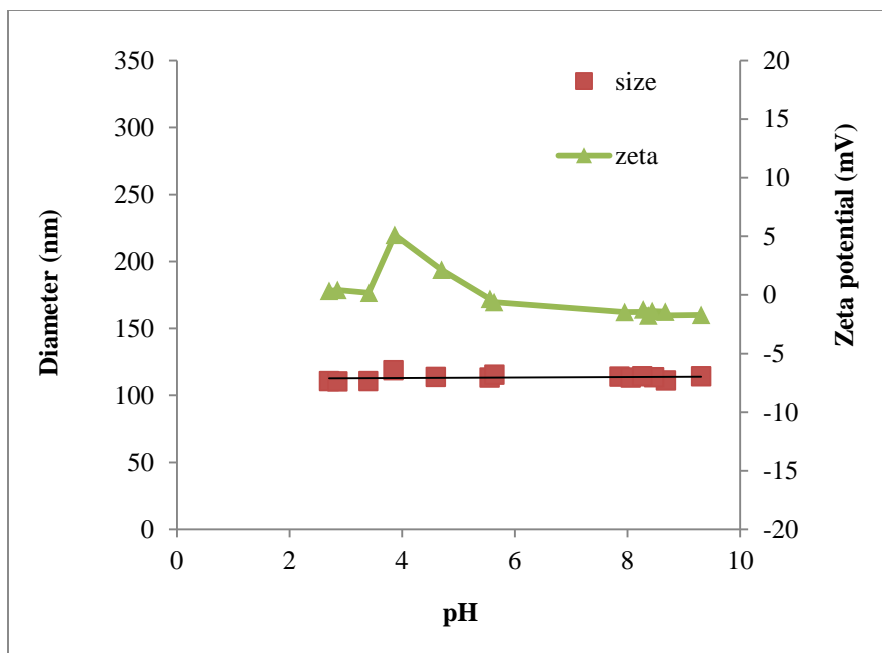


Figure 3.2. The change in size (nm) and zeta potential (mV) of PLGA (α T) NPs was measured with respect to changing pH showing, a 4 nm increase in size from pH 2.5-9, from 110 nm – 114 nm in diameter.

PLGA-Chi particles showed similar stability under changing pH conditions. These particles increased slightly more in size than the PLGA nanoparticles did, but the size increase was only from 116 nm to 162 nm (Figure 3.3). The effect of zeta potential on size was more apparent for the PLGA-Chi NPs than for the PLGA NPs. As the zeta potential approached neutrality with increasing pH, the size of the PLGA-Chi NPs increased (Figure 3.3) (Table 3.1). This was expected because stronger zeta potentials (negative or positive) typically indicate stronger repulsion between particles, and thus smaller sizes.

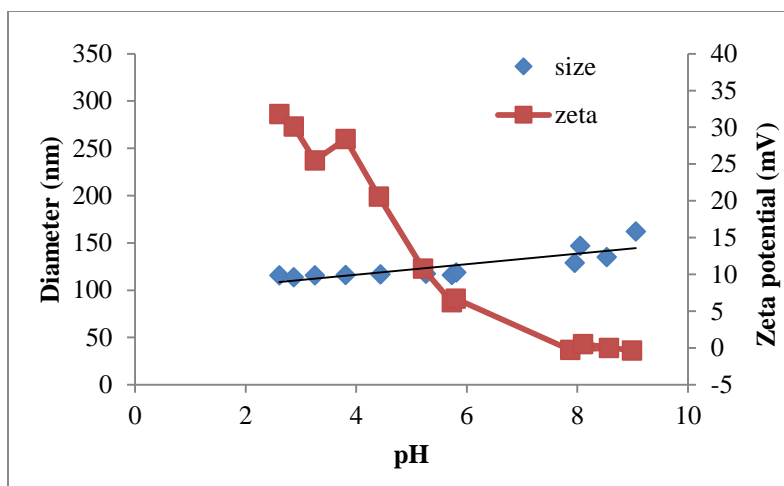


Figure 3.3. The change in size (nm) and zeta potential (mV) of PLGA-Chi (α T) NPs was measured with respect to changing pH. In acidic conditions, when the the zeta potential was 32 mV, the size was 116 nm. The size and zeta potential reached 162 nm and -0.34 mV in basic conditions.

Table 3.1 summarizes the physical properties including size and zeta potential of PLGA and PLGA-Chi NPs represented in Figures 3.1-3.3.

		DI Water (pH 5.5)	Gastric environment (pH 2)	Intestinal Environment (pH 7)
PLGA NPs	size (nm)	97.82 \pm 2.63	110.3	114
	zeta (mV)	-36.2 \pm 1.31	0.345	-1.72
PLGA-Chi NPs	size (nm)	134.1 \pm 2.05	116	129-147
	zeta (mV)	38 \pm 2.90	31.8	-0.229

3.4.4 Alpha-tocopherol Chemical Stability

Knowledge of stability of the α T entrapped in the particles when in simulated GI environments is necessary to understand the fate of the nanodelivered α T *in vivo*, especially when determining bioavailability. The results of the chemical stability experiment showed no degradation of α T in the particles during the 3 hours they were exposed to the gastric environment. From time 0 to 3 hours, 100% of the entrapped α T was detected (Figure 3.4).

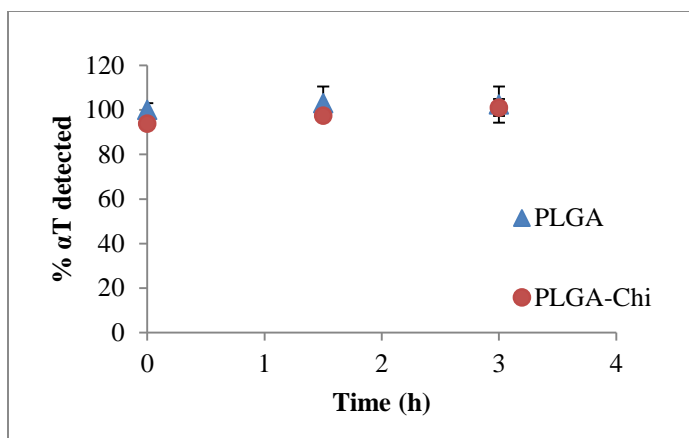


Figure 3.4. The total α T present was measured when PLGA and PLGA-Chi NPs were exposed to a simulated gastric environment for 3 hours, and 100% of the initial α T was detected after 3 hours.

The results of the chemical stability of α T in the simulated intestinal environment mirrored that of the stability in the gastric environment. The particles provided protection of the α T from degradation during the time frame of analysis (48 h) (Figure 3.5).

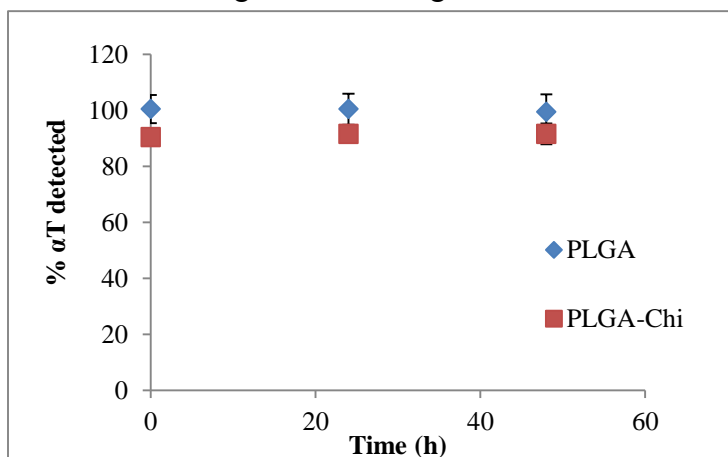


Figure 3.5. The total α T present was measured when PLGA and PLGA-Chi NPs were exposed to a simulated intestinal environment for 48 hours, and 100% of the initial α T was detected after 48 hours.

3.4.5 Alpha-tocopherol Release Kinetics

The α T found outside of the particles in the gastric environment is shown in Figure 3.6. According to the data, approximately 5% of the entrapped α T was detected outside of the NP at time 0. Three hours later, no more α T had been released from either PLGA or PLGA-Chi NPs.

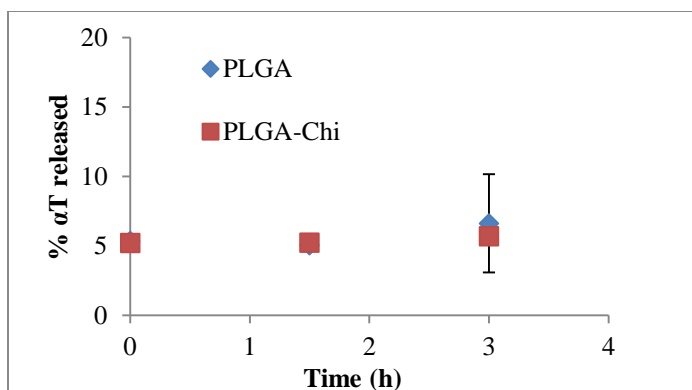


Figure 3.6. PLGA and PLGA-Chi NPs were exposed to a simulated gastric environment for 3 hours, and percent of α T released was measured by HPLC over time. Both NP systems showed no release of α T between time 0 and 3 hours.

Immediately after the particles were suspended in the intestinal media, approximately 5% of the associated α T was detected outside of the NPs. After 72 hours of exposure to the intestinal media, the 95% entrapped α T remained in the PLGA and PLGA-Chi particles. The release kinetics showed no differences in behavior between PLGA and PLGA-Chi under these conditions (Figure 3.7).

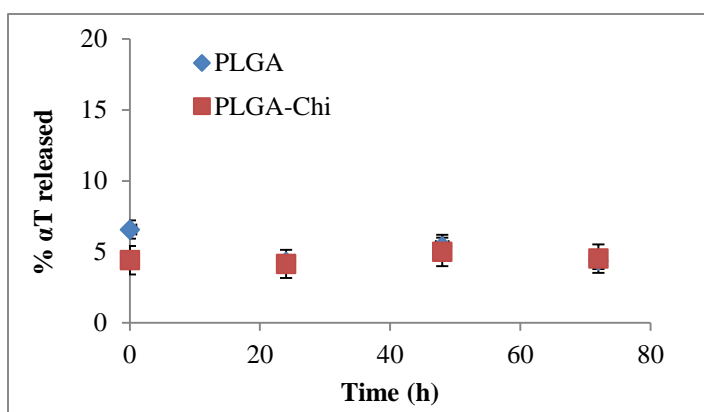


Figure 3.7. PLGA and PLGA-Chi NPs were exposed to a simulated intestinal environment for 72 hours, and percent of α T released was measured by HPLC over time. After 72 hours, the amount of α T detected outside the particles had not increased since time 0.

3.4.6 Pharmacokinetic profile

PLGA and PLGA-Chi NPs were designed to enhance the oral bioavailability of lipophilic bioactives. Moreover, α T was used as a model drug not only to determine ability of the NPs to improve bioavailability, but also the ability of the mucoadhesive properties of PLGA-Chi NPs to improve bioavailability when compared to PLGA NPs alone. After an acute administration of 1.5 mg α T delivered in PLGA NPs, PLGA-Chi

NPs, and in free form, the concentration of α T in the plasma was measured and plotted in terms of time (Figure 3.8).

Free α T showed a rapid uptake and clearance after administration. The C_{\max} was 2.91 $\mu\text{g/ml}$ and occurred at a T_{\max} of 8 hours following oral gavage. At 12 hours, the plasma concentration of free α T was approaching the baseline. On the other hand, both NP-delivered systems showed a distinct uptake pattern compared to the free α T. At two hours after administration, an increase in plasma concentration was evident, but four hours later, the concentration of α T delivered by both NP systems increased to over 3 $\mu\text{g/ml}$ (Figure 3.8). These values stayed constant over the following 8 hours, where the PLGA NP-delivered α T measured 3.35 $\mu\text{g/ml}$ plasma and the PLGA-Chi NP-delivered α T measured 3.9 $\mu\text{g/ml}$ plasma 12 hours following administration (Figure 3.8). Twenty-four hours after administration, plasma concentration of α T delivered by both NP systems was decreasing. This decrease continued until baseline levels of α T were reached by α T delivered by both PLGA and PLGA-Chi NPs (Figure 3.8).

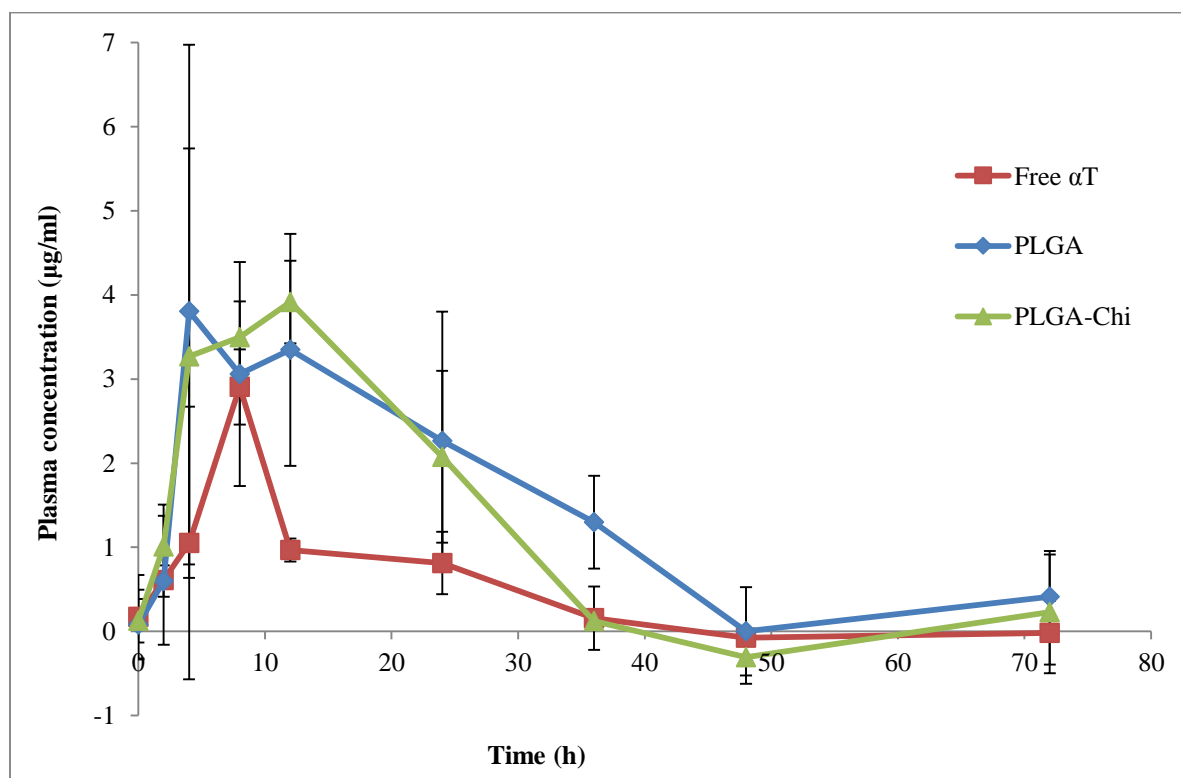


Figure 3.8. The pharmacokinetic parameters were obtained when the rat plasma concentrations ($\mu\text{g/ml}$) of α T delivered in PLGA, PLGA-Chi, and in free form were plotted as a function of time (n=3). The concentrations were detected using positive ion mass spectroscopy.

From the plasma concentration-time curve, AUC was obtained for each of the three curves (Table 3.2). The AUC for the control was 36.64 $\mu\text{g/ml/h}$. The AUC for the αT delivered by PLGA NPs and PLGA-Chi NPs were 99.0 $\mu\text{g/ml/h}$ and 80.92 $\mu\text{g/ml/h}$, respectively. According to these values, the bioavailability of the treatment delivered by PLGA was 170% higher than the control. Similarly, the bioavailability of the bioactive delivered in PLGA-Chi NPs was improved by 121% compared to the free αT . These values illustrate that both NP systems significantly improve bioavailability of lipophilic bioactives when orally delivered in rats, but PLGA-Chi NPs do not improve the bioavailability when compared with PLGA NPs under these conditions.

Table 3.2. The pharmacokinetic parameters of T_{max} , C_{max} , and AUC were obtained for both treatments and the control from the plasma concentration-time curve (Figure 3.8) using NCSS 9 version 9.0.7 (NCSS, LLC. Kaysville, UT, USA). *There was no statistical difference between these values.

Treatment	T_{max} (h)	C_{max} ($\mu\text{g/ml}$)	AUC ($\mu\text{g/h/ml}$)
Free αT	8	2.91	36.64
PLGA NPS	4-12*	3.81	99.00
PLGA-Chi NPS	12	3.92	80.93

3.5 Discussion

Particle behavior and *in-vivo* fate of nanodelivered bioactives is not a result of one, isolated parameter, rather it is heavily influenced by the interdependence of many parameters such as nanoparticle characteristics (e.g. size, surfactant, zeta potential), type of bioactive (e.g. hydrophobic or hydrophilic), and media to which exposed (e.g. gastric, intestinal, blood).

Immediately following freeze-drying, the physical characteristics of PLGA and PLGA-Chi NPs showed similarities in size but differences in zeta potential. Specifically, they measured 97.87 ± 2.63 nm and 134.1 ± 2.05 nm for PLGA and PLGA Chi NPs, respectively. In terms of zeta potential, PLGA NPs were very negatively charged (-36 ± 1.31 mV) and PLGA-Chi NPs were very positively charged (38 ± 2.9 mV) when suspended in DI water at pH approximately 5.5. Although differences in the particles were apparent in water, when the particles were exposed to GI conditions, the varying characteristics changed in a way that made both PLGA and PLGA-Chi NPs very similar. For example, when the particles were exposed to pH changes mimicking GI transit, the size in the gastric environment was 110 nm for PLGA NPs and 116 nm for PLGA-Chi NPs (Table 3.1). The zeta potential of the PLGA NPs became neutral (0.345 mV), but the zeta potential of the PLGA-Chi NPs remained strong (31.8 mV). The major characteristic separating the two NP systems when freshly made and suspended in water—zeta potential--was no longer a factor under intestinal conditions. The zeta potentials of both

particle systems reached neutrality, measuring -1.72 mV (PLGA NPs) and -0.229 mV (PLGA-Chi NPs) in conditions with intestinal pH (Table 3.1). Because of the neutral zeta potential of the PLGA-Chi NPs, an increase in size from 116 nm to 129-147 nm was evident (Table 3.1). Further, we saw no difference in protection of α T when both PLGA and PLGA-Chi NPs were exposed to simulated gastric and intestinal conditions over 48 hours. Both particle systems were synthesized using the same amount of PVA, which in addition to the PLGA matrix proved to be protective of NP degradation in simulated GI environments.

Release of the entrapped bioactive from PLGA NPs has been reported as a “diffusion-cum-degradation-mediated” process. This means that during the early stages, release occurs via diffusion through the polymer matrix. In the later phases, the release occurs by both diffusion through the matrix and degradation of the matrix itself (Panyam et al., 2003). Over the time frame of this experiment, it was apparent that release was in the early stages of the diffusion phase and no degradation occurred, as supported by others as well (Cai et al., 2003; Panyam et al., 2003). Alpha-tocopherol is a very non-polar compound, and its tendency to diffuse out from inside the lipophilic matrix of PLGA into a polar environment is not likely. In addition, PVA has been shown to provide a strong barrier against degradative molecules penetrating the PLGA matrix. (Grama et al., 2011; Panyam et al., 2003).

The physical and chemical characteristics of PLGA and PLGA-Chi NPs featured in this study aid in understanding the behavior of the NP systems *in vivo*. The analysis of the bioavailability data (Figure 3.8) was approached with the *in vitro* findings in mind. It was apparent that α T was protected by the NP systems in the simulated GI environments and no α T was released from the particles between time 0 and 3h (gastric) and 0 and 72 h (intestinal). From these findings, it must be concluded that the α T was shuttled to the intestinal barrier in entrapped form. From this data, it is impossible to determine the physical condition of the particles as they cross the intestinal barrier and reach systemic circulation. The NPs could either be endocytosed by the enterocytes, transcytosed through the enterocytes, transported paracellularly, or taken up by the M cells of the Peyers’ Patches found in the gut associated lymphoid tissue (Italia et al., 2011). Regardless of the route to systemic circulation, it cannot be concluded from this data whether the α T detected in the plasma was free or still physically entrapped by the NP.

The goal of this study was to determine if PLGA and PLGA-Chi NPs improved the bioavailability of lipophilic antioxidants (α T) by reducing variable absorption and if the mucoadhesive properties of chitosan improved this bioavailability even further than PLGA NPs. The PK profile in Figure 3.8 confirmed that nano-delivery improves bioavailability of α T by more than 100% ($p < 0.05$). Further, when we compared the AUC of α T delivered in PLGA and PLGA-Chi NPs to that of freely delivered α T, the relative bioavailability of α T was 270% and 220%, respectively. No statistical difference was found between the PLGA and PLGA-Chi delivered α T ($p > 0.05$).

Similar results on improved bioavailability were seen in other studies using PLGA NPs as a delivery system. Estradiol-loaded PLGA NPs orally delivered in rats showed a 9-fold improvement in bioavailability and T_{\max} of 12-32 h depending on the molecular weight of the particle, compared to a T_{\max} of 2 h when estradiol was delivered in free form (Mittal et al. 2007). Similarly, curcumin-loaded PLGA NPs delivered in rats showed an improved bioavailability of 15.6-fold compared to freely administered curcumin. The T_{\max} of the NP-delivered curcumin was 2 h, while the freely delivered curcumin was 0.5h (Khalil et al. 2012). Cyclosporine was no exception when delivered by PLGA NPs. When 15 mg/kg body weight was delivered to rats, the NP-delivered drug showed a 19% higher absorption than the commercially-available drug Sandimmune Neoral®. Perhaps this increase was not as significant as previously reported in the literature because Sandimmune Neoral contains cyclosporine in the form of a microemulsion, which has shown better uptake capability than free form (Italia et al. 2007). While the NPs did not show a significant improvement in bioavailability of cyclosporine, they did significantly change the PK profile of the drug. Moreover, the T_{\max} of the NP delivered cyclosporine was 24 h, while the commercially available dose was 2 h after oral administration. This published data combined with the current study on α T infers that PLGA NPs not only improved the bioavailability of poorly absorbed drugs, but they also significantly changed the pharmacokinetic profile of the drug.

The bioavailability of α T delivered in PLGA NPs was 270% of the control α T; this improvement was seen in other α T delivery systems. For example, α T-loaded Capectinate microcapsules increased bioavailability compared to free α T by 118% in rats (Song et al. 2009). AT bioavailability was improved by 200% in gelucire 44/14 products in humans (Barker et al 2003). By the same token, a nano-emulsion system increased bioavailability of α T by 260% in rats (Hatanaka et al. 2010). Although it seems redundant to have many delivery systems accomplishing the same goal, we must keep in mind that α T serves as a model bioactive to determine the efficacy of PLGA as a nanodelivery system. From the results of this study, we see that not only are PLGA and PLGA-Chi NPs efficient drug carriers, but they offer an abundance of advantages over other delivery systems in addition to improving bioavailability. Unlike other delivery systems, polymeric nanoparticles like PLGA are capable of protecting the entrapped drug from the GI environment, they can be tailored to desired release properties, and they are geared towards the size-dependent uptake suited to the intestinal membrane. PLGA NPs are a versatile, practical, and effective delivery system for hydrophobic bioactives with poor bioavailability.

Chapter 4 Conclusions and Future Work

4.1 Conclusions

Polymeric nanoparticles such as PLGA were proposed to address challenges in delivery of poorly absorbed drugs. The first step in determining the effectiveness of PLGA NPs as a delivery system was discovering nanoparticle accumulation and elimination *in vivo*. Because of the popularity of PLGA NPs as delivery systems in medical research, there was enough data to compile biodistribution trends of PLGA NPs *in vivo* into a comprehensive review paper. The most important trends extracted from the data included the following: 1. Minimal amounts of NPs reached the brain and heart, and of the NPs that did reach these organs, rapid clearance was evident. 2. Higher nanoparticle presence was detected when physically entrapped indicators (dyes, fluorophors, entrapped drugs, etc.) were measured rather than covalently linked indicators. 3. Concentration of nanoparticles in various organs was higher in intravenously delivered NPs than orally-delivered NPs of similar properties. 4. Published data on orally-delivered PLGA NPs was minimal.

The lack of data on orally delivered PLGA NPs presented an opportunity to investigate the ability of PLGA NPs to improve bioavailability of a model hydrophobic bioactive (α T) when delivered orally in rats. In addition, it was an opportunity to improve upon PLGA NPs' ability to shuttle drugs by adding chitosan, a mucoadhesive compound, on the surface of the particles. The results indicated that both particle systems were able to improve the bioavailability of the α T by over 200%. However, PLGA-Chi NPs did not improve bioavailability of the α T delivered over that delivered by PLGA NPs. This was likely due to the similar properties of PLGA and PLGA-Chi NPs under simulated intestinal environment, where absorption occurs. Through the bioavailability study, the effectiveness of PLGA NPs to improve bioavailability of an entrapped bioactive was demonstrated. PLGA NPs were proven eligible as a delivery systems that can protect the bioactive from degradation by preventing release and maintaining its size stability in GI conditions which are advantages of polymeric nanodelivery systems.

4.2 Future Work

In order for PLGA nanodelivery systems to be employed as a suitable drug-delivery vehicle, more questions should be answered in addition to physical stability of the particles and chemical stability of the entrapped bioactive.

1. Biodistribution is one of the most critical parameters to understand before a NP can be used commercially as a drug delivery system. Since it was concluded that physically entrapped indicators are not as accurate as a covalently-linked indicator, more data on biodistribution with orally-delivered covalently-linked PLGA NPs is needed.
2. Nanoparticle-drug association is still unknown *in vivo*. To determine particle association, a proper method of detection would be needed. Covalently-linked

indicators such as TRITC could be used to track particle biodistribution in parallel with model drug distribution.

3. Dose-response of orally-administered PLGA NPs is a missing piece of the puzzle that would be of great advantage to future use of PLGA NPs as a drug delivery system. Specifically, it is unknown what the saturation point of NPs in the intestines would be.
4. There is an evident separation in understanding between cell studies and *in vivo* studies. When the data from these two studies, using the same NP system, is compared, it is typically conflicting. We as researchers need to breach the gap in order to determine how the NPs are transported from the intestinal wall into systemic circulation and how NP properties affect this pathway.

References

- Acharya S, Sahoo SK. (2011). PLGA NPs containing various anticancer agents and tumour delivery by EPR effect. *Adv Drug Delivery Rev.* 63(3): 170-183.
- Acharya G, Shin CS, Vedantham K, McDermott M, Rish T, Hansen K, Fu F, Park K. (2010). A study of drug release from homogenous PLGA microstructures. *J Controlled Release.* 146(2): 201-206.
- Aggarwal P, Hall JB, McLeland CB, Dobrovolskaia MA, McNeil SE. (2009). NP interaction with plasma proteins as it relates to particle biodistribution, biocompatibility and therapeutic efficacy. *Adv Drug Delivery Rev.* 61(6): 428-437.
- Barker SA. (2003). An investigation into the structure & bioavailability of α -tocopherol dispersions in Gelucire 44/14. *J Controlled Release.* 91(3): 477-488.
- Beletsi A, Panagi Z, Avgoustakis K. (2005). Biodistribution properties of NPs based on mixtures of PLGA with PLGA-PEG diblock copolymers. *Int J Pharm.* 298: 233-241.
- BjØrneboe A. G. BjØrneboe, C. A. Drevon. (1990). Absorption, Transport and Distribution of Vitamin E. American Institute of Nutrition.
- Brenner GM, Stevens CW. (2009). Pharmacology. Philadelphia, PA: Saunders Elsevier.
- Cai Q, Shi G, Bei J, Wang S. (2003). Enzymatic degradation behavior and mechanism of poly (lactide-co-glycolide) foams by trypsin. *Biomaterials.* 24: 629-638.
- Cartiera MS, Johnson KM, Rajendran V, Caplan MJ, Saltzman WM. (2009). The uptake and intracellular fate of PLGA NPs in epithelial cells. *Biomaterials.* 30: 2790-2798.
- Cohn W. (1997). Bioavailability of Vitamin E. *Eur J Clin Nutr.*
- Danhier F, Ansorena E, Silva JM, Coco R, Le Breton A, Preat V. (2012). PLGA-based NPs: An overview of biomedical applications. *J Controlled Release* 161(2): 505-522.
- Fredenberg S, Wahlgren M, Reslow M, Axelsson A. (2011). The mechanisms of drug release in poly (lactic-co-glycolic acid)-based drug delivery systems-a review. *Int J Pharm.* 415(1-2): 34-52.
- Gramma CN, Ankola D, Kumar M. (2011). Poly (lactide-co-glycolide) nanoparticles for peroral delivery of bioactives. *Curr Opin Colloid In.* 16: 238-245.

- Gaumet M, Vargas A, Gurny R, Delie F. (2008). NPs for drug delivery: The need for precision in reporting particle size parameters. *Eur J Pharma Biopharma*. 1: 45-52.
- Hatanaka J, Chikamori H, Sato H, Uchida S, Debari K, Onoue S, Yamada S. (2010). Physicochemical and pharmacological characterization of α -tocopherol-loaded nano-emulsion system. *Int J Pharm*. 396: 188-193.
- Italia JL, Bhatt DK, Bhardwaj V, Tikoo K, Ravi Kumar MNV. (2007). PLGA nanoparticles for oral delivery of cyclosporine: Nephrotoxicity and pharmacokinetic studies in comparison to Sandimmune Neoral®. *J Controlled Release*. 119: 197-206.
- Khalil NM, Sascimento TCF, Casa DM, Dalmolin LF, Mattos AC, Hoss I, Romano MA, Mainardes RM. (2013). Pharmacokinetics of curcumin-loaded PLGA and PLGA-PEG blend nanoparticles after oral administration in rats. *Colloid Surface B*. 101: 353-360.
- Li Y, Pei Y, Zhang X, Gu Z, Zhou Z, Yuan W, Zhou J, Zhu J, Gao X. (2001). PEGylated PLGA NPs as protein carriers: synthesis, preparation and biodistribution in rats. *J Controlled Release*. 71: 203-211.
- Lodge JK. (2005). Vitamin E bioavailability in humans. *J Plant Physiol*. 162.7: 790-796.
- Mittal G, Sahana DK, Bhardwaj V, Ravi Kumar MNV. (2007). Estradiol loaded PLGA nanoparticles for oral administration: Effect of polymer molecular weight and copolymer composition on release behavior in vitro and in vivo. *J Controlled Release*. 119: 77-85.
- Mondal N, Halder KK, Kamila MM, Debnath MC, Pal TK, Ghosal SK, Sarkar BR, Ganguly S. (2010). Preparation, characterization, and biodistribution of letrozole loaded PLGA NPs in Ehrlich Ascites tumor bearing mice. *Int J Pharm*. 397: 194-200.
- Mouse Phenome Database. The Jackson Laboratory. [Online] Available at: <http://phenome.jax.org/>. Accessed 4 March 2012.
- Murugesu A, Astete C, Leonardi C, Morgan T, Sabliov C. (2011). Chitosan/PLGA particles for controlled release of α -tocopherol in the GI tract via oral administration. *Nanomedicine*.
- Owens D E, Peppas NA. (2006). Opsonization, biodistribution, and pharmacokinetics of polymeric NPs. *Int J Pharm*. 307(1): 93-102.
- Panyam J, Dali MM, Sahoo SK, Ma W, Chakravarthi S, Amidon GL, Levy RJ, Labhasetwar V. (2003). Polymer degradation and in vitro release of a model

- protein from poly (D,L-lactide-co-glycolid) nano- and microparticles. *J Controlled Release*. 92: 173-187.
- Parveen S, Sahoo SK. (2011). Long circulating chitosan/PEG blended PLGA NP for tumor drug delivery. *Eur J Pharmacol*. 670: 372-383.
- Phillips MA, Vargas A, Gran ML, Peppas NA. (2010). Targeted nanodelivery of drugs and diagnostics. *Nanotoday*. 5(2): 143-159.
- Plapied L. (2011). Fate of polymeric nanocarriers for oral drug delivery. *Curr Opin Colloid In*. 16: 228-237.
- The Rat Phenome Database [Online] Available at: http://www.anim.med.kyoto-u.ac.jp/nbr/strainsx/ow_list.aspx. Accessed 4 March 2012.
- Saxena V, Sadoqi M, Shao J. (2006). Polymeric nanoparticulate delivery system for Indocyanine green: Biodistribution in healthy mice. *Int J Pharm*. 308: 200-204.
- Snehalatha M, Venugopal K, Saha RN, Babbar AK, Sharma RK. (2008). Etoposide Loaded PLGA and PCL NPs II: Biodistribution and Pharmacokinetics after Radiolabeling with Tc-99m. *Drug Deliv* 15: 277-287.
- Song Y, Lee J, Lee HG. (2009). α -Tocopherol-loaded Ca-pectinate microcapsules: Optimization, *in vitro* release, and bioavailability. *Colloid Surface B*. 73: 394-398.
- Tobío M, Sánchez A, Vila A, Soriano I, Evora C, Vila-Jato JL, Alonso MJ. (2000). The role of PEG on the stability in digestive fluids and *in vivo* fate of PEG-PLA NPs following oral administration. *Colloid Surface B*. 18: 315-323.
- Tosi G, Vergoni AV, Ruozi B, Bondioli L, Badiali L, Rivasi F, Constantino L, Forni F, Vandelli MA. (2010). Sialic acid and glycopeptides conjugated PLGA NPs for central nervous system targeting: *In vivo* pharmacological evidence and biodistribution. *J Controlled Release*. 145: 49-57.
- Tsai Y, Jan W, Chien C, Lee W, Lin L, Tsai H. (2011). Optimized nano-formulation on the bioavailability of hydrophobic polyphenol, curcumin, in freely-moving rats. *Food chem*. 127: 918-925.
- Vergoni AV, Tosi G, Tacchi R, Vandelli MA, Bertolini A, Constantino L. (2009). NPs as drug delivery agents specific for CNS: *in vivo* biodistribution. *Nanomedicine* 5: 369-377.
- Yang Y, McClements DJ. (2013). Vitamin E Bioaccessibility: Influence of Carrier Oil Type on Digestion and Release of Emulsified α -Tocopherol Acetate. *Food Chem*.

Yin Y, Chen D, Qiao M, Wei X, Hu H. (2007). Lectin-conjugated PLGA NPs loaded with thymopentin: *Ex vivo* bioadhesion and *in vivo* biodistribution. J Controlled Release. 123: 27-38.

Zigoneanu IG, Astete CE, Sabliov CM. (2008). Nanoparticles with entrapped α -tocopherol: synthesis, characterization, and controlled release. Nanotechnology. 19.

Appendices

Appendix A Particle Characterization

Table A.1 The physical properties of size, zeta potential, and PDI were measured by DLS when freshly made particles were suspended in DI water at 25 °C.

Sample Name	size (nm)	PdI	ZP (mV)	size (nm)	PdI	ZP (mV)	size (nm)	PdI	ZP (mV)
PLGA NPs	100.9	0.11	-37.2	96.09	0.17	-36.6	96.63	0.18	-34.7
PLGA-Chi NPs	136.2	0.29	35.9	134	0.30	40.0	132.1	0.29	37.0

Table A.2. The calibration curve used for the in-vitro studies was generated using the listed concentrations, and areas were produced from fluorescent intensity using an excitation and emission of 290 nm and 330 nm, respectively.

Concentration (µg/ml)	Area under the curve
6	388.4
6	383.3
6	381.1
2	124.4
2	123.9
2	124
1	60.5
1	60.3
1	60.1
0.5	29.7
0.5	29.4
0.5	29.5
0.1	5.7
0.1	5.7
0.1	5.7

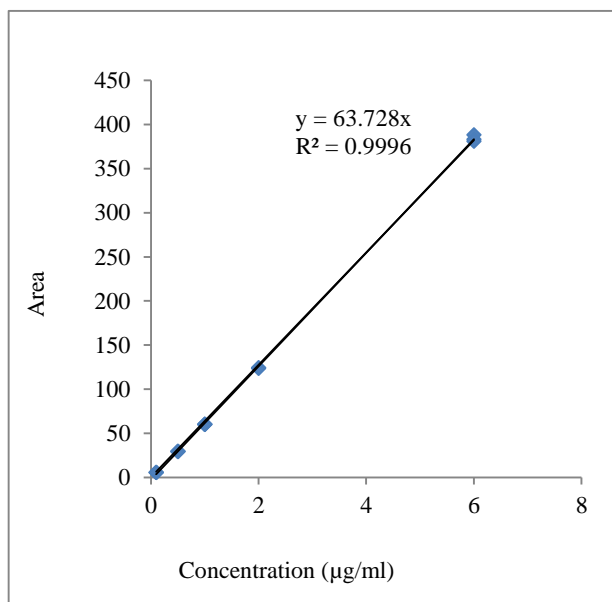


Table A.3. The concentration of α T per mg of powder from freshly made PLGA and PLGA-Chi NPs is represented in the table.

NP	AUC	Concentration in suspension (μ g/ml)	Concentration in particles (μ g α T/mg NP)
PLGA	237.5	3.73	24.84
PLGA	144.5	2.27	22.67
PLGA	177.4	2.78	27.84
PLGA-chi	126.1	1.98	19.79
PLGA-Chi	121.5	1.91	19.06
PLGA-Chi	125	1.96	19.61

Table A.4. The changes in size and zeta potential of PLGA and PLGA-Chi NPs when exposed to pH changes mimicking gastric and intestinal conditions as detected by DLS is shown.

PLGA NPs			PLGA-Chi NPs		
pH	Diameter (nm)	ZP (mV)	pH	Diameter (nm)	ZP (mV)
2.7	5.4	0.345	2.61	5.22	31.8
2.85	5.7	0.435	2.87	5.74	30.1
3.4	6.8	0.178	3.25	6.5	25.5
3.85	7.7	5.12	3.81	7.62	28.4
4.6	9.2	2.14	4.44	8.88	20.6
5.55	11.1	-0.334	5.26	10.52	10.8
5.64	11.3	-0.628	5.73	11.46	6.25
7.86	15.7	-1.47	5.81	11.62	6.71
8.68	17.4	-1.43	7.95	15.9	-0.229
8.47	16.9	-1.38	8.53	17.06	0.00392
8.26	16.5	-1.75	8.05	16.1	0.532
9.31	18.6	-1.72	9.06	18.12	-0.338

Table A.5. The chemical stability of α T entrapped in PLGA NPs in the gastric environment is shown.

Time (h)	Matrix	AUC	concentration in acetonitrile ($\mu\text{g/ml}$)	Actual concentration ($\mu\text{g aT/ml}$)	Total α T/sample ($\mu\text{g aT/ml}$)	Percent of starting α T
0	supernatant	22.5	0.35	7.06	138.58	97.42
0	supernatant	24.8	0.39	7.78	141.44	99.43
0	supernatant	25.3	0.40	7.94	147.09	103.40
0	pellet	419.1	6.58	131.52		
0	Pellet	425.9	6.68	133.66		
0	pellet	443.4	6.96	139.15		
1.5	supernatant	23.8	0.37	7.47	143.76	101.06
1.5	supernatant	21.2	0.33	6.65	137.74	96.83
1.5	supernatant	23.6	0.37	7.41	158.29	111.28
1.5	pellet	434.3	6.81	136.29		
1.5	pellet	417.7	6.55	131.08		
1.5	pellet	480.8	7.54	150.89		
3	supernatant	18.7	0.29	5.87	138.36	97.27
3	supernatant	23	0.36	7.22	139.71	98.22
3	supernatant	48.4	0.76	15.19	159.05	111.81
3	pellet	422.2	6.62	132.50		
3	pellet	404.1	6.34	126.82		
3	pellet	458.4	7.19	143.86		

Table A.6. The chemical stability of α T entrapped in PLGA-Chi NPs in the gastric environment is shown.

Time (h)	Matrix	AUC	Concentration in acetonitrile ($\mu\text{g/ml}$)	Actual concentration ($\mu\text{g } \alpha\text{T/ml}$)	Total $\alpha\text{T/sample}$ ($\mu\text{g } \alpha\text{T/ml}$)	Percent of starting αT
0	supernatant	24.3	0.38	7.64	6.81	4.79
0	supernatant	22.9	0.36	7.20	6.70	4.71
0	supernatant	23.6	0.37	7.42	6.58	4.62
0	pellet	408.9	6.43	128.58		
0	pellet	403.4	6.34	126.86		
0	pellet	394.8	6.21	124.15		
1.5	supernatant	24.3	0.38	7.64		
1.5	supernatant	22.2	0.35	6.98	6.85	4.82
1.5	supernatant	24.6	0.39	7.74	7.06	4.96
1.5	pellet		0.00	0.00		
1.5	pellet	413.6	6.50	130.06		
1.5	pellet	424.4	6.67	133.46		
3	supernatant	26.3	0.41	8.27	7.49	5.26
3	supernatant	26.1	0.41	8.21	7.21	5.07
3	supernatant	25.2	0.40	7.92	6.95	4.88
3	pellet	449.8	7.07	141.45		
3	pellet	432.3	6.80	135.94		
3	pellet	416.6	6.55	131.01		

Table A.7. The chemical stability of α T entrapped in PLGA NPs in the intestinal environment is shown.

Time (h)	Matrix	AUC	Concentration in acetonitrile ($\mu\text{g/ml}$)	Actual concentration ($\mu\text{g aT/ml}$)	Total α T/sample ($\mu\text{g aT/ml}$)	Percent of starting α T
0	pellet	440.9	6.92	138.36	148.12	104.09
0	pellet	401	6.29	125.84	134.66	94.63
0	pellet	434.7	6.82	136.42	145.90	102.53
0	supernatant	31.1	0.49	9.76		
0	supernatant	28.1	0.44	8.82		
0	supernatant	30.2	0.47	9.48		
24	pellet	451.3	7.08	141.63	147.81	103.87
24	pellet	447.3	7.02	140.37	147.06	103.34
24	pellet	408.3	6.41	128.13	133.66	93.93
24	supernatant	19.7	0.31	6.18		
24	supernatant	21.3	0.33	6.68		
24	supernatant	17.6	0.28	5.52		
48	pellet	445.5	6.99	139.81	150.29	105.62
48	pellet	402.8	6.32	126.41	132.25	92.93
48	pellet	430.2	6.75	135.01	141.69	99.57
48	supernatant	33.4	0.52	10.48		
48	supernatant	18.6	0.29	5.84		
48	supernatant	21.3	0.33	6.68		

Table A.8. The chemical stability of α T entrapped in PLGA NPs in the intestinal environment is shown.

Time (h)	Matrix	AUC	Concentration in acetonitrile (μ g/ml)	Actual concentration (μ g α T/ml)	Total α T/sample (μ g α T/ml)	Percent of starting α T
0	pellet	357	5.60	112.04	118.12	89.49
0	pellet	361.7	5.68	113.51	118.12	89.49
0	pellet	371	5.82	116.43	121.48	92.03
0	supernatant	19.4	0.30	6.09		
0	supernatant	14.7	0.23	4.61		
0	supernatant	16.1	0.25	5.05		
24	pellet	369.2	5.79	115.86	121.29	91.89
24	pellet	374.5	5.88	117.53	121.92	92.36
24	pellet	363.5	5.70	114.08	119.06	90.20
24	supernatant	17.3	0.27	5.43		
24	supernatant	14	0.22	4.39		
24	supernatant	15.9	0.25	4.99		
48	pellet	380.1	5.96	119.28	125.18	94.84
48	pellet	372.2	5.84	116.81	121.83	92.29
48	pellet	345.9	5.43	108.55	115.49	87.49
48	supernatant	18.8	0.29	5.90		
48	supernatant	16	0.25	5.02		
48	supernatant	22.1	0.35	6.94		

Table A. 9. PLGA (α T) release kinetics are shown as a function of time in the gastric environment.

Time (h)	Matrix	AUC	Concentration in acetonitrile ($\mu\text{g/ml}$)	Actual concentration ($\mu\text{g } \alpha\text{T/ml}$)	Percent αT released
0	supernatant	22.5	0.35	7.06	4.96
0	supernatant	24.8	0.39	7.78	5.47
0	supernatant	25.3	0.40	7.94	5.58
0	pellet	419.1	6.58	131.52	
0	pellet	425.9	6.68	133.66	
0	pellet	443.4	6.96	139.15	
1.5	supernatant	23.8	0.37	7.47	5.25
1.5	supernatant	21.2	0.33	6.65	4.68
1.5	supernatant	23.6	0.37	7.41	5.21
1.5	pellet	434.3	6.81	136.29	
1.5	pellet	417.7	6.55	131.08	
1.5	pellet	480.8	7.54	150.89	
3	supernatant	18.7	0.29	5.87	4.13
3	supernatant	23	0.36	7.22	5.07
3	supernatant	48.4	0.76	15.19	10.68
3	pellet	422.2	6.62	132.50	
3	pellet	404.1	6.34	126.82	
3	pellet	458.4	7.19	143.86	

Table A.10. PLGA-Chi (α T) release kinetics are shown as a function of time in the gastric environment.

Time (h)	Matrix	AUC	Concentration in acetonitrile ($\mu\text{g/ml}$)	Actual concentration ($\mu\text{g } \alpha\text{T/ml}$)	Percent αT released
0	supernatant	24.3	0.38	7.64	5.354947
0	supernatant	22.9	0.36	7.20	5.046432
0	supernatant	23.6	0.37	7.42	5.200689
0	pellet	408.9	6.43	128.58	
0	pellet	403.4	6.34	126.86	
0	pellet	394.8	6.21	124.15	
1.5	supernatant	24.3	0.38	7.64	5.354947
1.5	supernatant	22.2	0.35	6.98	4.892174
1.5	supernatant	24.6	0.39	7.74	5.421058
1.5	pellet		0.00	0.00	
1.5	pellet	413.6	6.50	130.06	
1.5	pellet	424.4	6.67	133.46	
3	supernatant	26.3	0.41	8.27	5.795683
3	supernatant	26.1	0.41	8.21	5.75161
3	supernatant	25.2	0.40	7.92	5.553278
3	pellet	449.8	7.07	141.45	
3	pellet	432.3	6.80	135.94	
3	pellet	416.6	6.55	131.01	

Table A.11. PLGA (α T) release kinetics are shown as a function of time in the intestinal environment.

Time (h)	Matrix	AUC	Concentration in acetonitrile ($\mu\text{g/ml}$)	Actual concentration ($\mu\text{g aT/ml}$)	Percent α T released
0	pellet	440.9	6.92	138.36	
0	pellet	401	6.29	125.84	
0	pellet	434.7	6.82	136.42	
0	supernatant	31.1	0.49	9.76	6.86
0	supernatant	28.1	0.44	8.82	6.20
0	supernatant	30.2	0.47	9.48	6.66
24	pellet	451.3	7.08	141.63	
24	pellet	447.3	7.02	140.37	
24	pellet	408.3	6.41	128.13	
24	supernatant	19.7	0.31	6.18	4.35
24	supernatant	21.3	0.33	6.68	4.70
24	supernatant	17.6	0.28	5.52	3.88
48	pellet	445.5	6.99	139.81	
48	pellet	402.8	6.32	126.41	
48	pellet	430.2	6.75	135.01	
48	supernatant	33.4	0.52	10.48	7.37
48	supernatant	18.6	0.29	5.84	4.10
48	supernatant	21.3	0.33	6.68	4.70
72	pellet	486.5	7.63	152.68	
72	pellet	478.7	7.51	150.23	
72	pellet	467	7.33	146.56	
72	supernatant	20.9	0.33	6.56	4.61
72	supernatant	22	0.35	6.90	4.85
72	supernatant	16.7	0.26	5.24	3.68

Table A. 12. PLGA-Chi (α T) release kinetics are shown as a function of time in the intestinal environment.

Time (h)	Matrix	AUC	Concentration in acetonitrile ($\mu\text{g/ml}$)	Actual concentration ($\mu\text{g } \alpha\text{T/ml}$)	Percent αT released
0	Pellet	357	5.60	112.04	
0	Pellet	361.7	5.68	113.51	
0	Pellet	371	5.82	116.43	
0	Supernatant	19.4	0.30	6.09	5.12
0	Supernatant	14.7	0.23	4.61	3.88
0	Supernatant	16.1	0.25	5.05	4.25
24	Pellet	369.2	5.79	115.86	
24	Pellet	374.5	5.88	117.53	
24	Pellet	363.5	5.70	114.08	
24	Supernatant	17.3	0.27	5.43	4.56
24	Supernatant	14	0.22	4.39	3.69
24	Supernatant	15.9	0.25	4.99	4.19
48	Pellet	380.1	5.96	119.28	
48	Pellet	372.2	5.84	116.81	
48	pellet	345.9	5.43	108.55	
48	Supernatant	18.8	0.29	5.90	4.96
48	supernatant	16	0.25	5.02	4.22
48	Supernatant	22.1	0.35	6.94	5.83
72	Pellet	356.1	5.59	111.75	
72	Pellet	351.4	5.51	110.28	
72	pellet	336.4	5.28	105.57	
72	Supernatant	19.8	0.31	6.21	5.22
72	Supernatant	15.8	0.25	4.96	4.17
72	Supernatant	15.9	0.25	4.99	4.19

Appendix B Pharmacokinetic Data

Table B.1. The calibration curve generated from the HPLC-MS is shown.

α T concentration ($\mu\text{g/ml}$)	α T area	dT area	ratio (α T/dT)
2	7160541	235100	30.45742663
2	7184827	233000	30.83616738
2	7690457	234217	32.83475153
1	3379365	236573	14.28466055
1	3417733	222070	15.39034088
1	3028783	203328	14.89604481
0.5	1827819	212698	8.593494062
0.5	1782156	211103	8.442115934
0.5	1588754	214409	7.409922158
0.1	666610	182978	3.643115566
0.1	601293	160117	3.755335161
0.1	outlier		
0.05	479416	141270	3.393615063
0.05	417037	119547	3.488477335
0.05	454088	109100	4.162126489

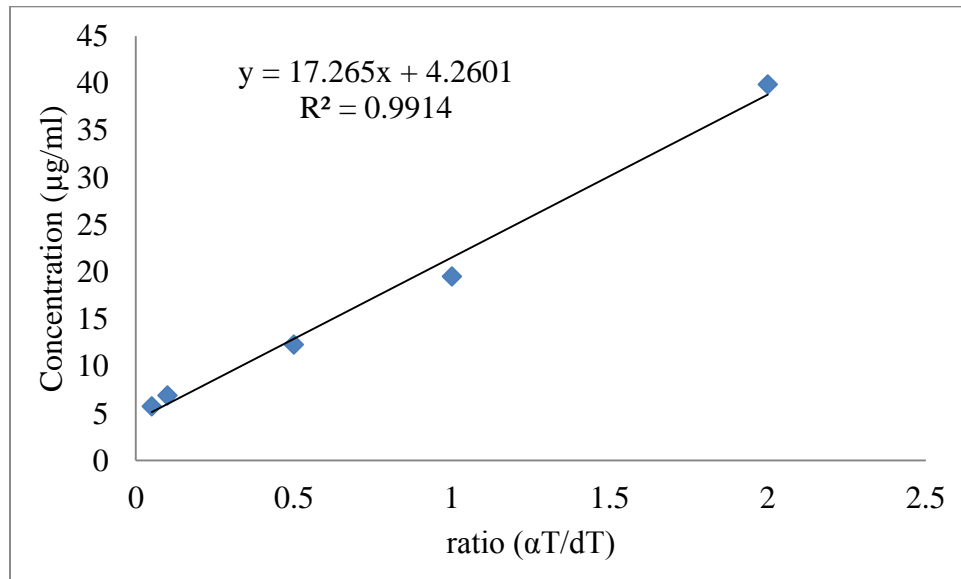


Table B. 2. The pharmacokinetic data from α T delivered in PLGA NPs is shown. The concentrations of α T detected in the plasma is reported as an output of HPLC-MS, using the ratio of the area of α T/dT to determine concentration.

Time (h)	ID	α T area	dT area	Ratio	Conc. in solution (μ g/ml)	Concentration in plasma (μ g/ml)
0	p1	319558	118070	2.707	-0.010	-0.199
0	p2	230484	71753	3.212	0.019	0.380
0	p3	328541	111791	2.939	0.003	0.067
0	p4	390066	142167	2.744	-0.008	-0.156
0	p5	96106	26150	3.675	0.046	0.910
0	p6	90085	28173	3.198	0.018	0.363
2	p1	149752	45336	3.303	0.024	0.484
2	p2	133812	37252	3.592	0.041	0.815
2	p3	184348	55625	3.314	0.025	0.497
4	p4	193213	50829	3.801	0.053	1.054
4	p5	449428	80479	5.584	0.155	3.095
4	p6	575824	62361	9.234	0.364	7.271
8	p1	164308	32916	4.992	0.121	2.417
8	p2	184014	38525	4.776	0.109	2.170
8	p3	191705	27823	6.890	0.229	4.589
12	p4	210258	40010	5.255	0.136	2.718
12	p5	200829	40371	4.975	0.120	2.397
12	p6	170320	23695	7.188	0.247	4.930
24	p1	121327	29300	4.141	0.072	1.443
24	p2	196398	48733	4.030	0.066	1.316
24	p3	163915	25574	6.409	0.202	4.039
36	p4	81430	18052	4.511	0.093	1.866
36	p5	152458	42983	3.547	0.038	0.763
36	p6	214613	53845	3.986	0.063	1.265
48	p1	291595	119915	2.432	-0.026	-0.513
48	p2	229252	68643	3.340	0.026	0.526
48	p3	188444	67754	2.781	-0.006	-0.113
72	p4	182553	49372	3.698	0.047	0.936
72	p5	123379	38587	3.197	0.018	0.363
72	p6	131552	46507	2.829	-0.003	-0.059

Table B.3. The pharmacokinetic data from α T delivered in PLGA-Chi NPs is shown. The concentrations of α T detected in the plasma is reported as an output of HPLC-MS, using the ratio of the area of α T/dT to determine concentration.



Time (h)	ID	α T area	dT area	Ratio	Conc. in solution (μ g/ml)	Concentration in plasma (μ g/ml)
0	c1	165290	56572	2.922	0.002	0.048
0	c2	333502	97032	3.437	0.032	0.637
0	c3	164739	55039	2.993	0.006	0.129
0	c4	233390	84786	2.753	-0.007	-0.146
0	c5	146409	47884	3.058	0.010	0.203
0	c6	175241	57748	3.035	0.009	0.177
2	c1	104149	31033	3.356	0.027	0.545
2	c2	168415	39915	4.219	0.077	1.533
2	c3	140442	37848	3.711	0.048	0.951
4	c4					
4	c5	306620	72875	4.207	0.076	1.519
4	c6	481188	66237	7.265	0.251	5.018
8	c1	230614	41512	5.555	0.153	3.062
8	c2	227163	36052	6.301	0.196	3.915
8	c3	239327	40217	5.951	0.176	3.514
12	c4	307815	52522	5.861	0.171	3.411
12	c5	195076	29054	6.714	0.219	4.388
12	c6	203286	32116	6.330	0.197	3.948
24	c1	100829	22553	4.471	0.091	1.821
24	c2	216540	38153	5.676	0.160	3.199
24	c3	101880	25896	3.934	0.060	1.206
36	c4	188545	61501	3.066	0.011	0.213
36	c5	136310	46838	2.910	0.002	0.035
36	c6	112290	37562	2.989	0.006	0.125
48	c1	195817	69764	2.807	-0.004	-0.084
48	c2					
48	c3	93379	38658	2.416	-0.027	-0.532
72	c4	182903	66336	2.757	-0.007	-0.141
72	c5	136720	51141	2.673	-0.012	-0.236
72	c6	216058	56692	3.811	0.053	1.066

Table B.4. The pharmacokinetic data from α T delivered in free form is shown. The concentrations of α T detected in the plasma is reported as an output of HPLC-MS, using the ratio of the area of α T/dT to determine concentration.

Time (h)	ID	α T area	dT area	Ratio	Conc. in solution (μ g/ml)	Concentration in plasma (μ g/ml)
0	f1	147841	51447	2.874	0.000	-0.007
0	f2	307979	127188	2.421	-0.026	-0.525
0	f3	114877	31676	3.627	0.043	0.854
0	f4	318347	100535	3.167	0.016	0.328
0	f5	142526	43383	3.285	0.023	0.464
0	f6	151487	43972	3.445	0.032	0.647
2	f1	176139	42174	4.176	0.074	1.484
2	f2	94811	30282	3.131	0.014	0.287
2	f3	100793	34426	2.928	0.003	0.055
4	f4	279683	115917	2.413	-0.027	-0.535
4	f5	226559	60655	3.735	0.049	0.979
4	f6	298929	57010	5.243	0.135	2.705
8	f1	256692	49495	5.186	0.132	2.639
8	f2	171808	33016	5.204	0.133	2.659
8	f3	223061	37993	5.871	0.171	3.423
12	f4	104249	27924	3.733	0.049	0.977
12	f5	123203	32080	3.840	0.055	1.099
12	f6	144347	40102	3.599	0.041	0.823
24	f1	149697	45406	3.297	0.024	0.477
24	f2	160855	40859	3.937	0.060	1.209
24	f3	144661	40915	3.536	0.038	0.750
36	f4	175425	58066	3.021	0.008	0.162
36	f5	129749	43077	3.012	0.008	0.151
36	f6	109567	30563	3.585	0.040	0.807
48	f1	225784	78297	2.884	0.000	0.004
48	f2	130627	47036	2.777	-0.006	-0.118
48	f3	83821.000	30188.000	2.777	-0.006	-0.118
72	f4	229277.000	71001.000	3.229	0.020	0.400
72	f5	135061.000	52258.000	2.585	-0.017	-0.338
72	f6	147226.000	52951.000	2.780	-0.006	-0.114

Appendix C Permission to Publish

Permission for use of published papers, figures, and tables from Copyright Clearance Center (Rightslink®).



[My Orders](#) [My Library](#) [My Profile](#) Welcome Isimo14@tigers.lsu.edu [Log out](#)

[My Orders](#) > [Orders](#) > [All Orders](#)

License Details

Thank you very much for your order.

Click [here](#) for Payment Terms and Conditions.


[Get a printable version for your records.](#)

Questions? Contact RightsLink's publicationservices@copyright.com

License Number	3365470702833
License date	Apr 10, 2014
Licensed content publisher	Informa Healthcare
Licensed content publication	Drug Metabolism Reviews
Licensed content title	The effect of nanoparticle properties, detection method, delivery route and animal model on poly(lactic-co-glycolic) acid nanoparticles biodistribution in mice and rats
Licensed content author	Lacey C. Simon, Cristina M. Sabliov
Licensed content date	Dec 5, 2013
Type of Use	Dissertation/Thesis
Volume number	46
Issue number	02
Start page	128
End page	142
Requestor type	Author
Format	electronic
Portion	Full article
Will you be translating?	no
Number of copies	50
Order reference number	None
Title of your thesis / dissertation	Bioavailability of alpha-tocopherol orally delivered with Poly(lactic-co-glycolic) acid (PLGA) and PLGA-Chitosan nanoparticles
Expected completion date	Mar 2014
Estimated Size (pages)	100
Total	0.00 USD

[Back](#)

Copyright © 2014 Copyright Clearance Center, Inc. All Rights Reserved. [Privacy statement](#) . Comments? We would like to hear from you. E-mail us at [info@copyright.com](#)



My Orders > Orders > All Orders

My Orders

Orders

Billing History

Payable Invoices

SEARCH

☒ Date Range: From To

☐ Order Number:

Go

View: ☐ All ☒ Completed ☒ Canceled ☒ Denied ☒ Credited ☒ Pending

Filter

Results: 1-6 of 6

Order Date	Article Title	Publication	Type Of Use	Order Status	Order Number
10-Apr-2014	The effect of nanoparticle properties, detection method, delivery route, and animal model on poly(lactic-co-glycolic) acid nanoparticles biodistribution	Drug Metabolism Reviews	Dissertation/Thesis	Completed	3365470702833
17-Mar-2014	Physicochemical and pharmacological characterization of α -tocopherol-loaded nano-emulsion system	International Journal of Pharmaceutics	reuse in a thesis/dissertation	Completed	3351450809893
17-Mar-2014	α -Tocopherol-loaded Ca-pectinate microcapsules: Optimization, <i>in vitro</i> release, and bioavailability	Colloids and Surfaces B: Biointerfaces	reuse in a thesis/dissertation	Completed	3351440262920
17-Mar-2014	PLGA nanoparticles for oral delivery of cyclosporine: Nephrotoxicity and pharmacokinetic studies in comparison to Sandimmune Neoral®	Journal of Controlled Release	reuse in a thesis/dissertation	Completed	3351431251933
17-Mar-2014	An investigation into the structure and bioavailability of α -tocopherol dispersions in Gelucire 44/14	Journal of Controlled Release	reuse in a thesis/dissertation	Completed	3351430871043
17-Mar-2014	Estradiol loaded PLGA nanoparticles for oral administration: Effect of polymer molecular weight and copolymer composition on release behavior <i>in vitro</i> and <i>in vivo</i>	Journal of Controlled Release	reuse in a thesis/dissertation	Completed	3351430645197

Vita

Lacey Simon obtained her undergraduate degree in Biological Engineering in December 2012 from Louisiana State University. She was an active member of the Biological Engineering Student Organization, Tau Beta Pi Engineering Honor Society, and Kappa Delta Sorority. Lacey worked for two years as an undergraduate researcher at Pennington Biomedical Research Center in the Transgenics Core before beginning her master's research. In August 2011, Lacey began her master's research which led to two published review papers focused on PLGA nanoparticle biodistribution and toxicity in rats and mice. The focus of her current work involved method development for oral delivery of polymeric nanoparticles with entrapped antioxidants and detection in plasma following delivery.

Lacey is a candidate for the degree of Master of Science in Biological and Agricultural Engineering from LSU in May 2014. Following graduation, Lacey will be employed by Proctor and Gamble as a manufacturing engineer in Pineville, Louisiana.